Response to Reviewer 1

Reviewer comments are in **bold**. Author responses are in plain text. Excerpts from the manuscript are in *italics*. Modifications to the manuscript are in *blue italics*. Page and line numbers in the responses correspond to those in the original ACPD paper.

Zaystev et al. report interesting experimental and mechanistic studies of products originated from the oxidation of toluene and 1,2,4-trimethylbenzene with OH radicals. The authors make use of several instruments based on chemical ionization coupled to high resolution mass spectrometry (CIMS and PTR). The experimental work is based on conducting photooxidation experiments, followed by the analysis of gas and particle phase products. The analysis is based on chemical ionization techniques in the gas phase using several reagent agents to target specific class of compounds. A complementary mechanistic work (kinetic model and Gamma kinetics parametrization) was used to model the experimental data. Although these experimental techniques provide powerful information about the formulas, they lack definitive structural information. I do have several concerns associated with the present manuscript:

We thank the reviewer for the input that helped us to improve the manuscript. The revised manuscript takes into account the comments and questions, as detailed in the responses below.

We break up comment 1 into individual sub-comments and respond to them separately.

1a. Clarity of the manuscript, the novelty, and the technical interpretation of the data. The authors need to do more through job to clearly describe the objective of the study. Why gas phase and particle phase were measured?

The objective of this study is to evaluate the importance of various gas-phase oxidation pathways of aromatic compounds in terms of production of oxygenated low-volatile species (including HOMs) and SOA formation potential. In response to the comment, we update the following sentence (P3 L5):

The goal of this work is to ~~We~~ identify gas-phase pathways leading to production of low-volatility compounds which are important for SOA formation and support these identifications with CIMS data and a method to characterize the kinetics of an oxidation system.

1b. In several occasion, I got lost and it was difficult to follow which instrument/reagent agent was used for what and why (a table in the SI will be beneficial for example)?

In a typical 1,2,4-TMB experiment 570 ions detected by NH_4^+ CIMS and 590 ions detected by H_3O^+ CIMS were enhanced during the experiment. Hence, we think that it would be overwhelming to include them as a table in SI. However, in response to the comment, we clarify which instrument and reagent ion were used throughout the manuscript:

P6 L24: *In the toluene experiments, the approximate yields of benzaldehyde and cresol (~0.10 and ~0.16, respectively) were calculated based on the decay of toluene measured by Vocus-2R-PTR-TOF, rise of the two products measured by PTR3 H_3O^+ CIMS and NH_4^+ CIMS (cresol was measured by H_3O^+ CIMS while NH_4^+ CIMS was used for detecting benzaldehyde), and accounting for losses of cresol and benzaldehyde from wall deposition and reaction with OH and NO_3 (Sect 2.4).*
P7 L2: *The kinetic model predictions for the two products agree within uncertainties with the ~~PTR-MS~~ H_3O^+*

CIMS measurements and the time series behaviour is again similar (Fig. 3b).
P7 L8: *The ~~observed~~ yields of these products observed with NH_4^+ CIMS are significantly smaller (~0.01 in both systems).*
P8 L33: *The total concentration of C_8 components predicted by MCM v3.3.1 for 1,2,4-TMB is in good agreement with the NH_4^+ CIMS and ~~PTR-MS~~ H_3O^+ CIMS measurements (less oxidized compounds (O:C < 0.25) were detected using H_3O^+ CIMS while NH_4^+ CIMS was used for more oxidized species), though the observed composition is distinctly different from the MCM prediction (Fig. 5).*

1c. The gas phase was conducted to help with mechanism, however the particle phase was also analyzed but was not discussed (why and how these particle species were formed: partitioning, heterogeneous chemistry…).

The goal of this study is to evaluate the importance of various gas-phase oxidation pathways of aromatic compounds in terms of SOA formation potential. In Section 3.3 "SOA Analysis" products detected in the particle phase are compared to those detected in the gas phase to further understand the mechanism of toluene and 1,2,4-TMB SOA formation (P10 L24).

1d. Organonitrates were mentioned but not discussed!

While we agree with the reviewer that organonitrates make up an important class of organic molecules in the atmosphere, discussing individual classes of atmospheric compounds lies beyond the scope of this manuscript. The goal of this study is rather to evaluate the importance of various gas-phase oxidation pathways leading to the formation of highly oxygenated, low-volatile compounds that might contribute to SOA formation.

1e. The uncertainties were not discussed here (see my minor comments).

Uncertainties of the used instrumentation are discussed in Section 2.2 (P4 L14-16).

1f. Toluene and 124-TMS were studied in the literature and several important studies were not reported/discussed (e.g. Kamens/Jang group on toluene, Kleindienst work, Laskin work etc..). Several papers report chemical species observed in toluene SOA and in ambient PM2.5 in several places around the world. Do these species were observed here?

We think it would be overwhelming to include all existing references on photooxidation of toluene, 124-TMB and other aromatic compounds in this short paper. We included what we thought were the most relevant references for understanding the significance of various oxidation pathways of aromatic hydrocarbons. In addition, Calvert et al. (2002) cited in the manuscript gives an excellent overview of the relevant literature prior to 2002. However, in response to this comment, we added a few additional references, including previous toluene photooxidation studies (P2 L14):

The OH-adducts can react with atmospheric O_2 through H-abstraction to form ring-retaining phenolic compounds (i.e., cresols and trimethylphenols) (Jang and Kamens, 2001; Kleindienst et al., 2004).

2. Another important point that need to be discussed by the authors: artefacts associated with these techniques mainly thermal degradations of polar compounds/side chemical reactions (see recent papers by Jimenez and P. Ziemann groups for example). I have provided two references below (some co-authors in this study were also associated with these artefacts studies: a. Xiaoxi Liu, Benjamin Deming, Demetrios Pagonis, Douglas A. Day, Brett B. Palm, Ranajit Talukdar, James M. Roberts, Patrick

R. Veres, Jordan E. Krechmer, Joel A. Thornton, Joost A. de Gouw, Paul J. Ziemann, and Jose L. Jimenez
b. Effects of gas–wall partitioning in Teflon tubing and instrumentation on time-resolved measurements of gas-phase organic compounds. Demetrios Pagonis, Jordan E. Krechmer, Joost de Gouw, Jose L. Jimenez, and Paul J. Ziemann

In response to the comment, we discuss three types of potential artefacts associated with CIMS technique: thermal degradation, fragmentation during ionization, and inlet losses.

a. During particle-phase measurements using TD-NH_4^+ CIMS and TD-H_3O^+ CIMS, sampled air passes through a gas-phase denuder (Ionicon Analytik GmbH, Austria), which removes the gas-phase organics, and then through a thermal desorption region heated to 180℃, in which the aerosol particles are vaporized. This may result in thermal decomposition of OVOCs. We studied thermal decomposition of OVOCs extracted from alpha-pinene SOA by measuring their peak intensities using TD-NH_4^+ CIMS. Signals of many species increased at moderate temperatures (T < 160℃) and levelled out or decreased at higher temperatures (T > 180℃), as shown in Fig. R1 (Zaytsev et al., 2019). Therefore, we chose TDU temperature to be 180℃, as at this temperature the major fraction of particles was evaporated while thermal decomposition of labile species was relatively small.

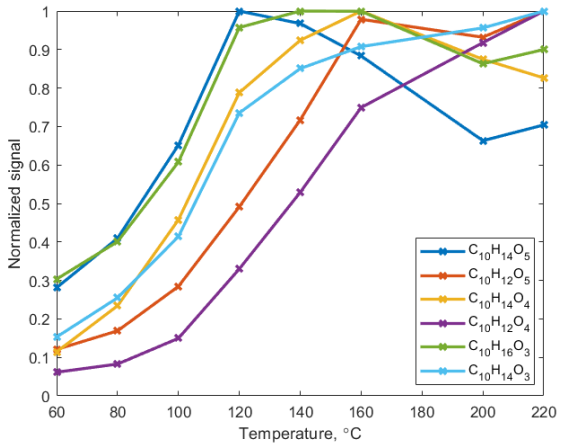

Figure R1: Thermograms of select OVOCs extracted from alpha-pinene ozonolysis SOA.

We modify the description of TD-NH_4^+ CIMS and TD-H_3O^+ CIMS (P4 L21):

Particle-phase compounds were quantified using the FIGAERO-HRToF-I^- CIMS (Lopez-Hilfiker et al., 2014), and a second PTR3 that could be operated in two positive modes as described above and equipped with an aerosol inlet comprising a gas-phase denuder and a thermal desorption unit heated to 180℃ (TD-NH_4^+ CIMS and TD-H_3O^+ CIMS). At this temperature, all particles were evaporated while thermal decomposition of labile oxygenated compounds was relatively small (Zaytsev et al., 2019).

b. Electric field strength within the CIMS instruments controls the amount of gas phase ion clustering and fragmentation which may lead to additional artefacts in the gas-phase data. Moderately strong fields are routinely used in H_3O^+ CIMS (E/N = 90 Td in PTR3 H_3O^+ CIMS) which may result in fragmentation of analyte molecules. In particular, large hydrocarbons including aromatic

compounds (C_8 and larger) are known to fragment to small common masses, while aldehydes and alcohols can lose H_2O (Erickson et al., 2014; Buhr et al., 2002). On the contrary, weaker fields are used in NH_4^+ CIMS (*E/N* = 60 Td in PTR3 NH_4^+ CIMS) and therefore result in smaller fragmentation comparing to H_3O^+ CIMS. Hence, PTR3 NH_4^+ CIMS was mainly used for detection of larger and more functionalized molecules (P4 L11).

c. The following discussion of inlet losses is included in the Supplement:

Inlet losses in CIMS instruments
Concentrations of gaseous analytes can be perturbed by gas-wall interactions occurring in the tubing used for sampling gases from the environmental chamber or inside the instruments. In order to estimate the response timescale of CIMS instruments (PTR3, Vocus, and I^- CIMS), we follow the procedure described in detail by Pagonis et al. (2017). At the beginning of the procedure, the instruments sampled air from the environmental chamber containing decane photooxidation products. Later, the instruments sampling lines were abruptly reconnected to zero air resulting in step-function decrease in the concentrations of the oxidation products. PTR3, Vocus and I^- CIMS time responding profiles measured in response to this step-function decrease were used to calculate delay times for the three instruments. Inlet delay times for all measured compounds did not exceed 20 seconds (Fig. S1).

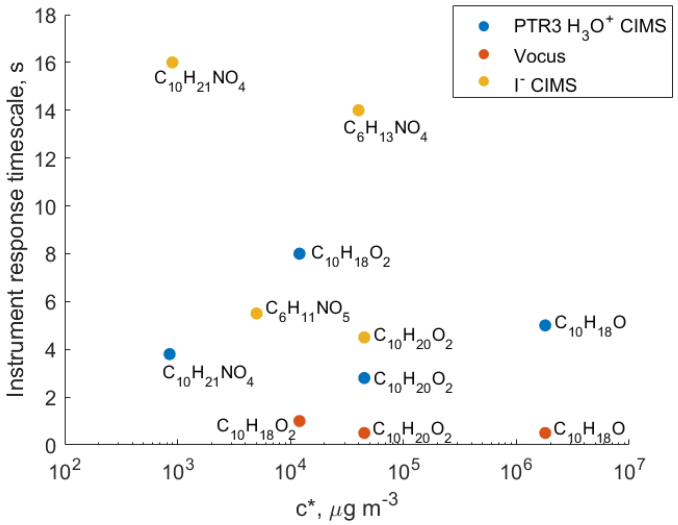

Figure S1: Measured instrument delay times as a function of SIMPOL c for CIMS instruments.*

The following sentence is changed (P4 L6):

PTR3 and Vocus-2R-PTR-TOF are designed to minimize inlet losses of sampled compound (Krechmer et al., 2018; Breitenlechner et al., 2017); for more details see the Supplement.

3. Given the analysis of gas and particle phase species in this work, it would be useful to include table(s) that outline partitioning coefficients of these species. A discussion will be beneficial here since gas and particle are linked together! How this study could be beneficial to urban atmosphere and the contribution of aromatic to ambient organic aerosol? Are these HOMs species important? While this study might provide valuable information for a better understanding of the chemical pathways from

the photooxidation of toluene and 124-TMB, the results presented here are not sufficiently discussed and/or do not present a real novelty (most products observed here were reported in the literature!).

Partitioning coefficients for low-volatile compounds could be obtained if the equilibrium between the gas and particle-phase organics was achieved. However, there are a number of reasons why simple gas-particle partitioning might not explain the concentrations observed in the two phases. First, chamber lights were turned on during the whole duration of experiments resulting in constant production and loss of oxidation products in the gas phase. Second, particles were lost on the chamber walls, while the wall loss term was not estimated. Third, CIMS and PTR-MS instruments cannot distinguish between isomers and do not provide further insight into the molecular structure of detected compounds. Hence, it is possible that several compounds with the same molecular formulas, but different structures and partitioning coefficients were lumped together. Therefore, partitioning coefficients for observed species cannot be reported.

While we agree with the reviewer that the majority of the observed products had been reported before, the goal of this study was to identify gas-phase pathways leading to production of low-volatility compounds which are important for SOA formation and support these identifications with CIMS data and a novel method to characterize the kinetics of an oxidation system.

Other comments.

1. Page 1, line 14. Change "A series of" with "eight" report how many experiment were conducted.

We change the sentence as suggested (P1 L14):

Four ~~A series of~~ toluene and four 1,2,4-trimethylbenzene (1,2,4-TMB) photooxidation experiments were performed in an environment chamber under relevant polluted conditions (NO_x ~ 10 ppb).

2. Page 1, line 17. Need to add the reagent chemicals used for the two PTRs to be consistent with the CIMS (e.g. H_3O^+ PTR, …).

Unlike CIMS instruments, which can use a variety of reagent ions to detect different classes of VOCs, PTR-MS instruments routinely use hydronium (H_3O^+) ions to ionize VOCs (Yuan et al., 2017). Hence, we think it would be excessive to include reagent ions used by the PTR-MS instruments in the abstract. This information, however, is included in Section 2.2 "Chamber Instrumentation" (P4 L2-4).

3. The end of the following sentence is hard to understand "An extensive suite of instrumentation including two Proton-Transfer Reaction Mass-Spectrometers (PTR-MS) and two Chemical Ionization Mass-Spectrometers (NH_4^+ CIMS and I^- CIMS) allowed for quantification of reactive carbon in multiple generations of oxidation"

In this study, we define "generation" as the number of reactions with OH (P6 L13). We change the sentence as following (P1 L16):

An extensive suite of instrumentation including two Proton-Transfer Reaction Mass-Spectrometers (PTR-MS) and two Chemical Ionization Mass-Spectrometers (NH_4^+ CIMS and I^- CIMS) allowed for quantification of reactive carbon in multiple generations of hydroxyl radical (OH)-initiated oxidation.

4. Page 2, line 5. Needs reference(s)

We include the following references (P2 L5):

Toluene, the most abundant alkylbenzene in the atmosphere, is primarily emitted by aforementioned anthropogenic processes (Wu et al., 2014).

5. Page 2, line 9-10. The authors state that 124-TMB is a good candidate (serve a model molecule) for substituted aromatic compounds? Please add reference(s) here and clarify this statement? This class of compounds behave widely differently vis-à-vis "chemistry, SOA production, OH rate constants…"

The most abundant aromatic species in the atmosphere are benzene, toluene, xylenes, ethylbenzene and trimethylbenzenes (Birdsall and Elrod, 2011). Among these species, trimethylbenzenes represent the most substituted aromatic compounds. In this study we compare and contrast gas-phase oxidation pathways leading to production of low-volatility compounds for less and more substituted aromatics (toluene and 1,2,4-TMB; P3 L1-2).

We change the sentence as suggested (P2 L9):

1,2,4-trimethylbenzene (1,2,4-TMB) is chosen ~~serves~~ as a model molecule to study oxidation of more substituted aromatic compounds (i.e., trimethylbenzenes).

6. Page 2, line 11. Delete "often"

We change the sentence (P2 L11):

In the atmosphere, oxidation of aromatic hydrocarbons is primarily ~~most often~~ initiated by their reactions with hydroxyl radicals (OH) via H-abstraction from the alkyl groups or OH addition to the aromatic ring.

7. Figure 1. Suggest adding a second panel on the right side associated with 124-TMB (similar to the toluene).

We include Figure 1 in this paper to illustrate four major oxidation pathways common for numerous aromatic compounds (including toluene and 1,2,4-TMB). Hence, we think it would be overwhelming to add 1,2,4-TMB oxidation scheme to this figure. However, in response to this comment, we change the title of Figure 1:

Figure 1: ~~Gas-phase chemical mechanism for toluene photooxidation.~~ Major gas-phase oxidation pathways for aromatic hydrocarbons, using toluene as an example. Reaction yields for the ~~major~~ oxidation pathways of toluene recommended by MCM v3.3.1 are shown in black. The proposed yields from the present study are shown in blue. The yield of the peroxide-bicyclic pathway is calculated based on the yields of ring-scission products.

8. Figure 2. Is the chemistry under low NO_x relevant here (either under the chamber conditions or under urban high NOx conditions)? Hydroperoxide channels are minor! The paper focusses on high NO_x! It is unlikely that these chemicals are formed under the conditions presented in this study. I suggest this figure should describes the chemistry relevant to the conditions reported in this study. There is a large number of such mechanisms reported in the literature?

We agree with the reviewer that the focus of this paper is the mechanistic study of highly oxygenated, low volatile products from oxidation of aromatic compounds under urban conditions. However, MCM v3.3.1 predicts than under studied conditions a non-negligible fraction of peroxy radicals reacts with HO_2

to produce hydroperoxides and carbonyls (Figs. S3 and S4). Therefore, it would be beneficial for the paper to keep the hydroperoxide channel in the Introduction and in Fig. 2. In addition, the formation of compounds with molecular formulas corresponding to hydroperoxides was observed in our experiments (P8 L5-6).

9. Page 2, lines 20-21. Delete the sentence associated with low NO_x.

As we mentioned in our response to the previous comment, MCM v3.3.1 predicts that under studied conditions the RO_2+HO_2 reaction can make up 5-10% of the bicyclic peroxy radical reactivity (Figs. S3 and S4). Hence, we think it would be beneficial to discuss all oxidation pathways in the Introduction. However, in response to the comment we change the order of the discussion starting with the reaction with NO and continuing with other reactions (P2 L20):

Under urban-relevant high-NO conditions BPRs also react with NO to form bicyclic oxy radicals that decompose to ring scission carbonylic products such as (methyl) glyoxal and biacetyl. Recent theoretical studies predict a new type of epoxy-dicarbonyl products that have not reported in previous studies (Li and Wang, 2014, Wu et al., 2014). Reaction of BPRs with NO can also result in formation of bicyclic organonitrates. In addition, ~~Under low-NO conditions~~, BPRs react with HO_2 and RO_2, forming bicyclic hydroperoxides and bicyclic carbonyls, respectively (Fig. 2). Finally, ~~In addition~~, BPRs can undergo unimolecular H-migration followed by O_2-addition (~~so-called~~ autooxidation) leading to the formation of non-aromatic ring-retaining highly oxygenated organic molecules (HOMs) (Bianchi et al., 2019). Molteni et al. (2018) reported elemental composition of the HOMs from a series of aromatic compounds produced under low-NO conditions. The autooxidation pathway might be more important for the substituted aromatics because of the higher yield of BPR formation and the larger number of relatively weak C-H bonds (Wang et al., 2017). ~~Under urban-relevant high-NO conditions BPRs also react with NO to form bicyclic oxy radicals that decompose to ring scission carbonylic products such as (methyl) glyoxal and biacetyl. Recent theoretical studies predict a new type of epoxy-dicarbonyl products that have not reported in previous studies (Li and Wang, 2014, Wu et al., 2014). Reaction of BPRs with NO can also result in formation of bicyclic organonitrates.~~

10. Please add "BPRs" to figures.

We add the notation "BPR" after "Bicylic peroxy radical" on Fig 1. Figure 2 depicts oxidation pathways of bicylic peroxy radicals, as mentioned in the title of the figure.

11. Please correct the title of Figure 2. Also in figures 1 and 2, references should be provided in the titles since the mechanism presented is not new to this study. Are the structures provided in Figure 2 experimentally determined in the literature? This should be stated clearly if these structures (mainly HOMs) were only proposed based on chemical formulas obtained from HR-CIMS/PTR and mechanism/computational chemistry.

We include references and update titles of Figs. 1 and 2 as suggested:

Figure 1: ~~Gas-phase chemical mechanism for toluene photooxidation.~~ Major gas-phase oxidation pathways for aromatic hydrocarbons using the example of toluene. Reaction yields for the toluene ~~major~~ oxidation pathways recommended by MCM v3.3.1 are shown in black (Bloss et al., 2005). The proposed yields from the present study are shown in blue. The yield of the peroxide-bicyclic pathway is calculated based on the yields of ring-scission products.

Figure 2: Oxidation pathways of bicyclic peroxy radicals in the OH-initiated oxidation of 1,2,4-trimehtylbenzene. The starting radical is shown in blue. Bimolecular reactions are from MCM v3.3.1 (Bloss et al., 2005) and Birdsall and Elrod (2011).

12. Page 3, line 1. Delete "the " in "…the detailed mechanism…" Please provide experimental evidence that NO_x level was 10 ppb.

We change the sentence as suggested (P3 L1):

In the present work, we investigate ~~the~~ detailed mechanisms of hydroxyl radical multigeneration oxidation chemistry of two aromatic hydrocarbons: toluene and 1,2,4-trimethylbenzene under moderately high ~~moderate~~, urban-relevant NO_x levels (~10 ppbv).

The detailed discussion of chamber conditions during experiments is given in Section 2.1 "Experimental design". As stated in Section 2.2, HONO+NO_x levels were measured by 42i NOx monitor (Thermo Fisher Scientific), and the sum of concentrations of HONO and NO_x concentration for a typical experiment is shown in Fig. S2. However, in response to the comment, we update the title of Fig. S2 to clarify that NO_2 concentration shown in the figure was estimated using MCM v3.3.1 and not measured directly:

Figure S2 ~~S1~~: (a) OH exposure, ~~and~~ (b) concentrations of O_3, NO_2, HONO+NO_x, and (c) temperature and RH for a typical photooxidation experiment. NO_2 concentration was estimated using F0AM (Wolfe et al., 2016) based on MCM v3.3.1 (Bloss et al., 2005).

13. Page 3, line 2. The chamber conditions were stated in several part of the text as high-NO_x conditions. Here they introduce "moderate". The description of the conditions should be consistent through out the text. It is confusing and arbitrary throughout the literature how high-NO_x and low-NO_x conditions are defined?

We agree with the reviewer that the terms "high-NO_x" and "low-NO_x" can be arbitrary, so we describe the chamber conditions as "high-NO" throughout the manuscript (e.g., P3 L13). In this work, we follow the definition of high-NO and low-NO chemistry regimes introduced by Seinfeld and Pandis (2016). At sufficiently high-NO levels, the primary chain terminating reaction for peroxy radicals is the RO_2 + NO. This condition is called high-NO. On the contrary, if the fate of peroxy radicals is not determined by their reaction with NO, the condition is called low-NO. Under our experimental conditions, the RO_2 + NO reaction is estimated to be the primary loss of bicyclic peroxy radicals (Figs. S3 and S4). Hence, we call these experiments high-NO. At the same time, NO_2 levels observed in the environmental chamber are relevant for urban conditions as NO_2 concentration in major European cities varies from 3-38 ppb (Hazenkamp-von Arx et al., 2004).

We clarify the definition of the high-NO regime in the manuscript (P3 L13):

We performed a series of photochemical experiments, in which toluene and 1,2,4-TMB were oxidized by ~~OH under high-NO conditions~~ (Table S1).-The experiments were carried out under high-NO conditions such that the fate of peroxy radicals was primarily determined by their reaction with NO (Seinfeld and Pandis, 2016).

We change the following sentence (P3 L1):

In the present work, we investigate ~~the~~ detailed mechanisms of hydroxyl radical multigeneration oxidation chemistry of two aromatic hydrocarbons: toluene and 1,2,4-trimethylbenzene under moderately high, ~~moderate~~ urban-relevant NO_x levels (~10 ppbv).

14. Page 3, lines 1-7. This section does not provide clearly the work conducted in this study. Either the experimental or the mechanistic work? Define that gas phase and particle phase were the focus. In some area of the paper it seems that only the gas phase products were measured and in some other parts the particle phase (SOA) were analyzed. Please clearly define that both gas phase and particle were analyzed using these two instruments running under different reagent chemicals to analyze a wide range of compounds. The CIMS was used to analyze particle phase.

In this work we focus on studying both gas- and particle-phase oxidation products: gas-phase products are discussed in Sections 3.1 and 3.2 while particle-products are discussed in Section 3.3.

In response to the comment, we edit the sentence describing the instrumentation used in this study and products studied here (P3 L4):

~~We use four high-resolution time-of-flight chemical ionization mass spectrometers (NH_4^+-CIMS, I^--CIMS and two PTR-MS) to characterize and quantify gas- and particle-phase oxidation products.~~ We use three chemical ionization mass spectrometry (CIMS) techniques (I^- reagent ion, NH_4^+ reagent ion, and H_3O^+ reagent ion) to characterize and quantify gas-phase oxidation products. In addition, NH_4^+ CIMS and I^- CIMS were used to detect particle-phase products.

15. Page 3, line 11, please provide the flow rate used to keep the chamber volume constant (this important for dilution)?

We include the clean air flow rate in the manuscript (P3 L11):

During experiments the environmental chamber was operated in the constant-volume ("semi-batch") mode, in which clean air (11-14 lpm) was constantly added to make up for instrument sample flow. ~~clean air was continuously added to the chamber to keep its volume constant.~~

16. Are the temperature and RH being constant throughout the experiment? When turning the light ON in general T and RH change due to reactions and heat from the UV lamps? Comment here. Time series of T and RH should be provided in Figure S1 top.

The chamber conditions were controlled at 20℃ and 2% relative humidity (P3 L12).

We update Figure S1 by adding an additional panel with temperature and relative humidity (panel c):

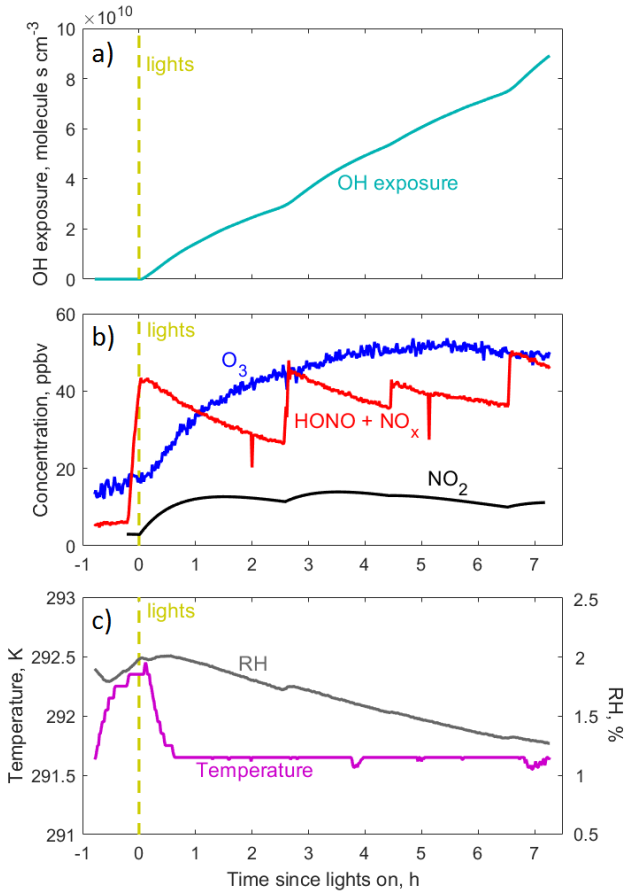

Figure S2 ~~S1~~: (a) OH exposure, ~~and~~ (b) concentrations of O_3, NO_2, HONO+NO_x, and (c) temperature and RH for a typical photooxidation experiment. NO_2 concentration was estimated using F0AM (Wolfe et al., 2016) based on MCM v3.3.1 (Bloss et al., 2005).

17. Page 3, line 13-14. "We performed a series of photochemical experiments, in which toluene and 1,2,4-TMB were oxidized by OH under high-NO conditions (Table S1)." Please provide NO_x (NO and NO_2) concentrations in Table S1. What the authors refers to high NO_x conditions? Provide references here!

In our experiments the sum of the concentrations of nitrogen oxides and HONO was measured by 42i NO_x monitor, and we modify the manuscript to make this clearer (P3 L29):

The concentration ~~of nitrogen oxides (NO_x) and HONO (42i NO_x monitor, Thermo Fisher Scientific),~~ ozone (2B Technologies), relative humidity, and temperature were measured in the chamber. A 42i NO_x monitor (Thermo Fischer Scientific) was used to measure the sum of concentrations of HONO and nitrogen oxides (NO_x).

Since individual levels of NO and NO_2 were not measured, they cannot be provided in Table S1. However, nitrogen oxides were primarily produced from HONO photolysis, and concentrations and time stamps of additional HONO injections are given in Table S1.

In this work we follow the definition of the high-NO chemistry regimes introduced by Seinfeld and Pandis (2016) (P3 L13):

We performed a series of photochemical experiments, in which toluene and 1,2,4-TMB were oxidized by ~~OH under high-NO conditions.~~ The experiments were carried out under high-NO conditions such that the fate of peroxy radicals was primarily determined by their reaction with NO (Seinfeld and Pandis, 2016).

At sufficiently high NO levels, the primary chain terminating reaction for peroxy radicals is the RO_2 + NO. This condition is called high-NO. On the contrary, if the fate of peroxy radicals is not determined by their reaction with NO, the condition is called low-NO. Under our experimental conditions, the RO_2 + NO reaction is the primary loss of bicyclic peroxy radicals (Figs. S3 and S4). Hence, these experiments are called high-NO. At the same time, NO_2 levels observed in the environmental chamber are relevant for urban conditions as NO_2 concentration in major European cities varies from 3-38 ppb (Hazenkamp-von Arx et al., 2004).

18. Please provide range of RH and T in Table S1 since term "approximative" was used.

During photooxidation experiments, the chamber conditions were controlled at 20℃ and 2% relative humidity. However, during experiments temperature and relative humidity slightly changed as shown in Fig. S1.

In response to the comment, we change the following sentence (P3 L12):

The temperature of the chamber was controlled at 292 (+/- 1) K. ~~and approximately 2% relative humidity~~. All experiments were carried out under dry conditions (relative humidity, RH ≅2%, +/-1%) to simplify gas- and particle-phase measurements. Higher RH can potentially shorten the lifetime of particle-phase hydroperoxides, epoxides, and organonitrates (Li et al., 2018) as well as affect gas-particle partitioning kinetics and thermodynamics (Saukko et al., 2012).

19. Page 3, line 14. "First, dry ammonium sulfate particles, used as condensation nuclei, were injected in the chamber reach a number concentration of (2.5 - 5.7)·10^4 cm^{-3}." Table S1, shows particle loading after seed injection in the order of (2.6 - 5.7)·10^4 cm^{-3} (no changes of the particle number after the light was ON and within the experimental error). Is this number stays the same throughout the experiment? Please clarify this in the footnote. This is important since HOMs were observed and will indicate if nucleation occurred or just growth of seed particles!! I'm curious how much aerosol mass was formed? - Table S1 should provide the amount of aerosol formed minus the seed aerosol injected. Specify the time of the reaction for these values? It is not stated in the manuscript that these values are associated with peak aerosol and compounds? - How much toluene was reacted? Since these experiments were conducted at low HC and NO_x concentrations, uncertainties should be discussed, and error bars should be provided for toluene and 124TMB. Providing time series in figure S1 top for example or in a separate figure will make the manuscript stronger?

The data is Table S1 corresponds to particle loading before the beginning of the experiment (i.e., before the lights were turned on). We add a footnote to Table S1 as suggested:

Particle loading was measured before the chamber lights were turned on.

In experiments #1-3 and 5-7, in which seed particles were injected, the total particle load decreased with time while organics to sulfate ratio increased (Fig. R2). Hence, low-volatile oxidation products produced in the chamber were primarily condensing on seed particles.

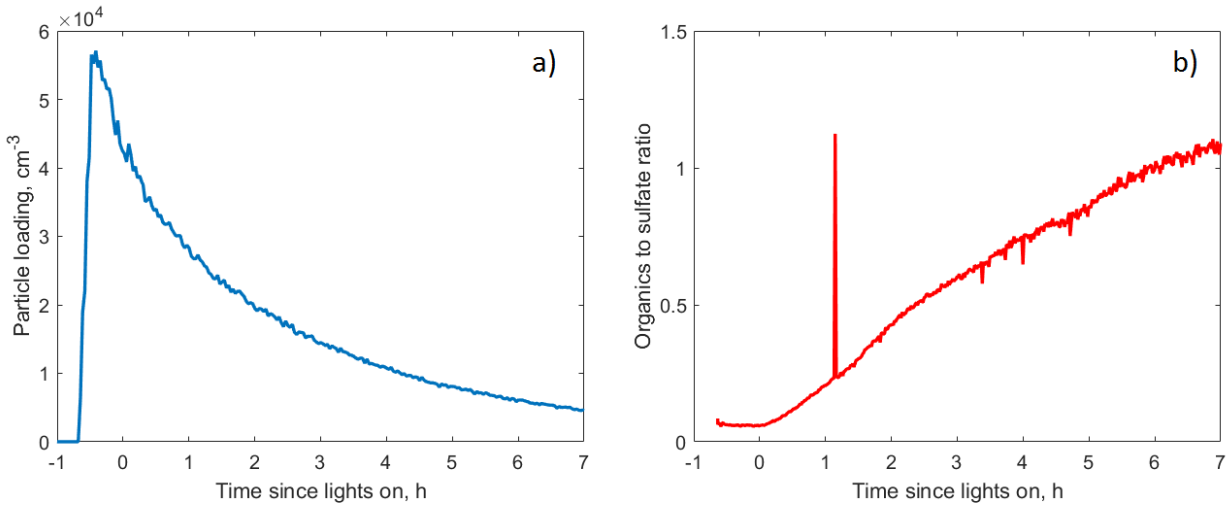

Figure R2: (a) Total particle loading measured by SMPS, and (b) organics to sulfate ratio measured by AMS in a 1,2,4-TMB photooxidation experiment.

On the contrary, in the experiments #4 and 8, in which no seed particles were injected, the total particle loading increased during the experiments (Fig. R3). This is an indication of nucleation happening in the chamber.

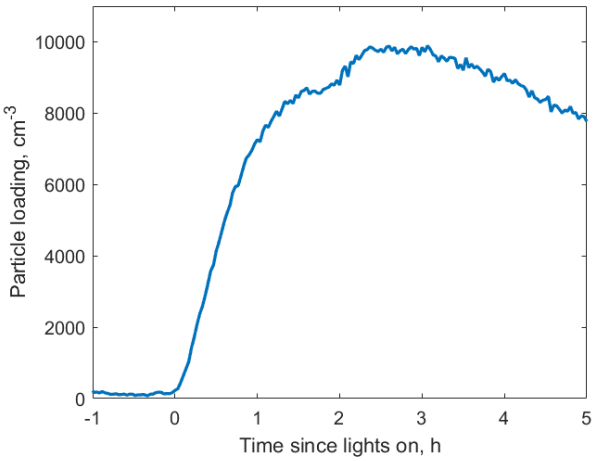

Figure R3: Total particle loading measured by SMPS in toluene photooxidation experiment #4, in which no seed particles were injected.

Total particle organics formed during experiments in this study was between 1.5-2 $\mu g/m^3$ as shown in Fig. 6.

In toluene experiments, 38-41 ppb of toluene was reacted over 5-6 hours of photooxidation. Uncertainties of the used instrumentation, including CIMS and PTR-MS instruments, are discussed in Section 2.2 (P4 L14-16).

20. Page 3, line 16-17. "Nitrous acid (HONO) was later injected as an OH precursor." It is not clear here! Table S1 shows that HONO was injected initially and during the experiment. Please clarify this statement? Please provide the source of NO in this section?

We change the following sentence (P3 L16):

Next, nitrous acid (HONO) was ~~later~~ injected as an OH precursor.

Additional aliquots of HONO were added to the chamber during experiments as stated in the manuscript (P3 L24).

We add the clarification on the source of NO (P3 L22):

The reagents were allowed to mix for several minutes, after which the ultraviolet (UV) lights, centered ~340 nm, were turned on to start photolysis of HONO (resulting in the production of hydroxyl radicals and nitric oxide) and photooxidation of the precursor.

21. Page 3, line 18-19. Data in Table S1 not consistent with the statement here? HONO in Table S1 was between 28 and 60 ppbv. Either Table S1 or the text needs to be corrected?

We change the sentence as suggested (P3 L18):

15 lpm of subsequently injected purified air carried HONO into the chamber, which resulted in a mixing ratio ~~concentration~~ of 28-35 ~~35-45~~ ppbv (except experiment 8 in which the initial HONO mixing ratio was 60 ppbv).

22. HONO was injected before the light was on. There is no background OH before the light was ON? Was the chamber in the dark before t=0? Figure S1 bottom shows background for NO_2, O_3, and HONO+NO_x? It is beneficial if C_6F_6 was presented also in Figure S1 top (dilution). - O_3 was high (~15 ppb) before light was ON! From where O_3 was generated before light ON?

The time stamp t=0 on Fig. S1 corresponds to the moment when the chamber lights were turned on. Hence, the lights were turned off before that moment. HONO photolysis, which results in production of OH and NO, began when the lights were turned on. Therefore, there was no source of OH in the dark chamber, and the background OH levels were negligible.

During experiments, the constant flow of clean air was added to the chamber, and hexafluorobenzene was used to monitor dilution (P3 L11). Hence, we think it would be overwhelming to include hexafluorobenzene tracer in Fig. S1. However, in response to the comment, we include it here (Fig. R4).

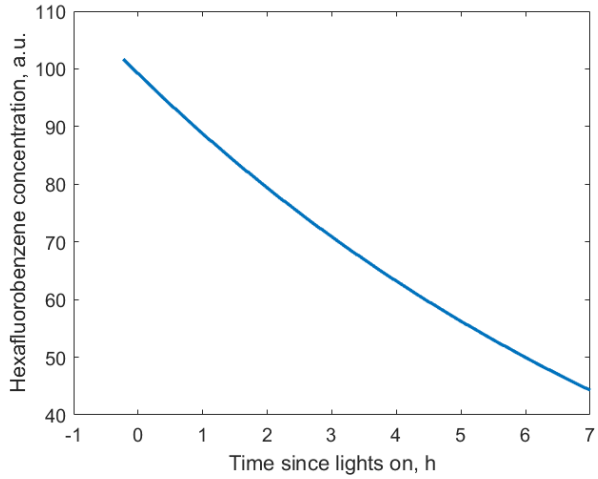

Figure R4: Concentration of hexafluorobenzene used as a dilution tracer in a typical photooxidation experiment.

We also include the total dilution over the course of each experiments in Table S1 and add the following sentence in the manuscript (P3 L16):

The total dilution over the course of experiments was 0.45-0.75 (except experiment 8 for which it was 0.27, Table S1).

Ozone background levels could be explained by the chamber contamination and the offset of the ozone monitor. In this paper, we aimed to study oxidation of aromatic compounds under relevant urban conditions, not ozone-free conditions. If the background ozone contributed to photochemistry during experiments, we can expect it to do the same thing in the real atmosphere as well. Hence, we did not aim to conduct experiments under ozone-free conditions.

23. "The concentration of NO in the chamber was estimated to be ~0.3 ppbv while NO_2 concentration was approximately 10 ppbv" I believe this is the initial concentration? In the manuscript the authors describe the experiments were conducted under high-NO? This is confusing? From this statement and Figure S1, the experiments were conducted under high NO_2? Please clarify this? How NO was estimated?

We include the clarification that the NO_x monitor was used to measure the sum of concentrations of NO_x and HONO (P3 L29):

The concentrations ~~of nitrogen oxides (NOx) and HONO (42i NOx monitor, Thermo Fischer Scientific),~~ ozone (2B Technologies), relative humidity, and temperature were measured in the chamber. A 42i NO_x monitor (Thermo Fischer Scientific) was used to measure the sum of concentrations of HONO and NO_x.

We did not measure individual concentrations of NO and NO_2 and used F0AM setup based on MCM v3.3.1 to estimate levels of these compounds. The concentrations of NO and NO_2 stated in the manuscript (0.3 and 10 ppb, respectively) correspond to the average values during experiments (Fig. R5).

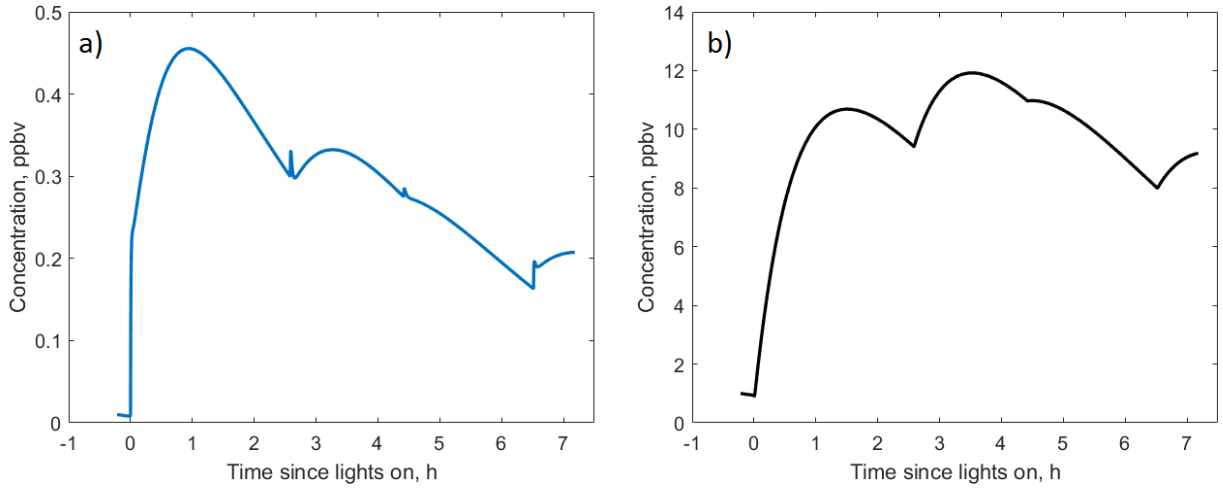

Figure R5: Estimated concentrations of NO and NO_2 during 1,2,4-TMB photooxidation experiment. Concentrations are estimated using F0AM setup based MCM v3.3.1.

In response to the comment we move the sentence towards the end of the section (P3 L19):

~~The concentration of NO in the chamber was estimated to be ~0.3 ppbv while NO_2 concentration was approximately 10 ppbv~~. After the addition of the oxidant, the aromatic precursor (toluene or 1,2,4-TMB, Sigma-Aldrich) was added to the chamber by injecting 3 µL of the precursor into a heated inlet. The initial concentration of the precursor was 89 ppbv in toluene experiments and 69 ppbv in 1,2,4-TMB experiments. The reagents were allowed to mix for several minutes, after which the ultraviolet (UV) lights, centred ~340 nm, were turned on to start photolysis of HONO and photooxidation of the precursor. During experiments, additional injections of HONO were added to the chamber in order to roughly maintain the OH levels. As a result, the mixing ratio of NO in the chamber during experiments was estimated to be ~0.3 ppbv while the NO_2 mixing ratio was approximately 10 ppbv (Fig. S2).

24. I suggest adding experiment ID in Table S1. Then, associate the experiment ID in each figure/table and where the data is discussed in the text? It is hard to link the origin of the data when discussed in the text figures and tables?

We add experiment IDs to Table S1 as suggested:

Table S1: Description of experiments.

Expt. no.	*VOC*	*Initial VOC concentration, ppbv*	*Initial HONO injection, ppbv*	*Additional HONO injections[a], ppbv*	*Particle loading after seed injection, cm^{-3}*	*Temp., K*	*RH, %*	*Total dilution*
1	*toluene*	*89*	*28*	*16 (124); 28 (220)*	*$2.6 \cdot 10^4$*	*292*	*2%*	*0.44*

2	*toluene*	*89*	*30*	*17 (140); 6 (180); 12 (290)*	*$4.2 \cdot 10^4$*	*292*	*2%*	*0.62*
3	*toluene*	*89*	*31*	*21 (125); 18 (290)*	*$3.2 \cdot 10^4$*	*292*	*2%*	*0.65*
4	*toluene*	*89*	*28*	*23 (180)*	*100[b]*	*292*	*3%*	*0.45*
5	*124-TMB*	*69*	*30*	*5 (155); 10 (300)*	*$3.6 \cdot 10^4$*	*292*	*2%*	*0.56*
6	*124-TMB*	*69*	*31*	*13 (145); 10 (245); 5 (345)*	*$3.8 \cdot 10^4$*	*292*	*2%*	*0.72*
7	*124-TMB*	*69*	*34*	*18 (150); 6 (265); 13 (390)*	*$5.7 \cdot 10^4$*	*292*	*2%*	*0.74*
8	*124-TMB*	*69*	*60*	*-*	*100[b]*	*292*	*2%*	*0.27*

[a] The following format is used: HONO injection in ppbv (time since the beginning of the experiment in min).
[b] Particle loading was measured before the chamber lights were turned on.

25. I'm confused with the term initial in Table S1. Are the authors referring before the light was ON? The system seems to be dynamic (clean air was continuously injected: dilution always occurring)" The initial concentrations of toluene and 1,2,4-TMB is very difficult to measure since the system was dynamic? I believe any quantitative data will be associated with high uncertainty? Provide error discussion in the manuscript! When conducting chamber experiments at low HC and NO_x concentrations, initial HCs and NO_x should be presented prior to light is ON and during the experiment. The instruments used should provide these data? Dilution data (C_6F_6) also should be provided in Figure S1?

At the beginning of each experiment (before the chamber lights were turned on), nitrous acid and aromatic precursor were injected in the chamber (P3 L16-21). The initial concentration of aromatic precursor is well-constrained since the amount of the precursor (3 μl) injected in the chamber, the chamber volume, and the rate of dilution were known. Vocus-2R-PTR was directly calibrated for toluene and 1,2,4-TMB, and the initial concentration measured by the instrument agreed well with the calculated value. Instrumentational uncertainties are discussed in Section 2.2 of the manuscript (P4 L14-16).

We include the total dilution over the course of each experiment in Table S1:

Table S1: Description of experiments.

Expt. no.	*VOC*	*Initial VOC concentration, ppbv*	*Initial HONO injection, ppbv*	*Additional HONO injections[a], ppbv*	*Particle loading after seed injection, cm^{-3}*	*Temp., K*	*RH, %*	*Total dilution*
1	*toluene*	*89*	*28*	*16 (124); 28 (220)*	*$2.6 \cdot 10^4$*	*292*	*2%*	*0.44*

2	*toluene*	*89*	*30*	*17 (140); 6 (180); 12 (290)*	*$4.2 \cdot 10^4$*	*292*	*2%*	*0.62*
3	*toluene*	*89*	*31*	*21 (125); 18 (290)*	*$3.2 \cdot 10^4$*	*292*	*2%*	*0.65*
4	*toluene*	*89*	*28*	*23 (180)*	*100[b]*	*292*	*3%*	*0.45*
5	*124-TMB*	*69*	*30*	*5 (155); 10 (300)*	*$3.6 \cdot 10^4$*	*292*	*2%*	*0.56*
6	*124-TMB*	*69*	*31*	*13 (145); 10 (245); 5 (345)*	*$3.8 \cdot 10^4$*	*292*	*2%*	*0.72*
7	*124-TMB*	*69*	*34*	*18 (150); 6 (265); 13 (390)*	*$5.7 \cdot 10^4$*	*292*	*2%*	*0.74*
8	*124-TMB*	*69*	*60*	*-*	*100[b]*	*292*	*2%*	*0.27*

[a] The following format is used: HONO injection in ppbv (time since the beginning of the experiment in min).
[b] Particle loading was measured before the chamber lights were turned on.

We also include the following sentence in the manuscript (P3 L16):

The total dilution over the course of experiments was 0.45-0.75 (except experiment 8 for which it was 0.27, Table S1).

26. Page 3, line 22-23. "The reagents were allowed to mix for several min, …" It is not clear if the chamber was mixed well (since no fans were used) before the start of the reaction (light ON?) It is not easy to conduct these kings of experiments: the chamber is always under dilution "continuously with clean air" at the same time injecting a known amount of reagents before the light is ON. It is necessary to provide the time series of all parameters measured and used to conduct the experiment? T, RH, HONO, HCs, SOA formed, C_6F_6… [Note, the amount of HC injected and the volume of the chamber does not provide accurate concentrations!] In general, HCs and HONO as well other reagents should be injected continuously in the chamber until a stable concentration is attained for all reagents, then stop the HC injection and turn ON the light (start of the reaction). Comments from the authors is need here! I do see the use of C_6F_6 to measure the dilution rate and it was discussed rarely in this paper.

The chamber mixing time can be calculated based on the aromatic precursor measured by Vocus-2R-PTR. After the precursor injection, we waited for a few minutes until the observed precursor level stabilized before turning the chamber lights on and starting the chemistry (P3 L22). Although no fans were used, we did not need them to keep the chamber well mixed: 11-14 slpm of clean air were constantly pushed into the chamber while the instruments were pulling ~7 slpm of air from the various points around the chamber, which resulted in turbulent mixing inside the chamber. In addition, mixing was promoted by fans external to the chamber blowing at the Teflon walls. As a result, the mixing time in the chamber was on the order of several minutes, which is much shorter than the duration of photooxidation experiments (several hours).

Time tracers of temperature, relative humidity, as well as concentrations of HONO+NO_x and O_3 are shown in Fig. S1. In addition, SOA formed in toluene and 1,2,4-TMB experiments is shown in Fig. 6. As we

discussed in our response to comment 22, we think it would be overwhelming to include the hexafluorobenzene tracer in Fig. S1, but we have included it in this document (Fig. R4).

The environmental chamber was operated in the constant-volume ("semi-batch") mode. In response to the reviewer's comment, we have edited the following sentence (P3 L11):

During experiments the environmental chamber was operated in the constant-volume ("semi-batch") mode, in which clean air (11-14 lpm) was constantly added to make up for instrument sample flow. ~~clean air was continuously added to the chamber to keep its volume constant.~~

27. Table S1. Particle loading should be (2.6 - 5.7) 10^4 instead of (2.6 - 3.5)10^4 as stated in line 15, page 1.

P3 L14-15 of the manuscript read:

First, dry ammonium sulfate particles were injected in the chamber to reach a number concentration of 2.5-5.7·10^4 cm^{-3}

28. Suggest using "Experimental section" instead of "Experimental design"

In our opinion, Section 2.1 provides the reader with the general description of conducted experiments (i.e., sequence in which various components were added to the chamber and operating conditions). As such, we think that the current title of this Section better describes its content.

29. Pages 3-4: chamber instrumentation. The description of the instruments is difficult to follow and switching between CIMS and PTR notations is hard to follow. All instruments use chemical ionization. At the beginning the authors state that four instruments were used (two CIMS and two PTR) and in this section it seems that three instruments were used: (1) page 4, line 1 ("including the I^- CIMS instrument; and two PTR (CIMS H_3O^+ and NH_4^+. This section needs to be clarified and consistent with the manuscript. Recently artefacts and sampling issues were reported, and this should be discussed in the paper (see my general comments).

We change the description of used instrumentation in Introduction (P3 L4):

~~We use four high-resolution time-of-flight chemical ionization mass spectrometers (NH_4^+-CIMS, I^--CIMS and two-PTR-MS) to characterize and quantify gas- and particle-phase oxidation products.~~ We use three chemical ionization mass spectrometry (CIMS) techniques (I^- reagent ion, NH_4^+ reagent ion, and H_3O^+ reagent ion) to characterize and quantify gas-phase oxidation products. In addition, NH_4^+ CIMS and I^- CIMS were used to detect particle-phase products.

We also change Section 2.2 (P3 L30):

~~Aromatic precursors as well as gas-phase oxygenated volatile organic compounds (OVOCs) were detected by chemical ionization high-resolution time-of-flight mass spectrometry (CIMS) instruments, including the I^--CIMS instrument (Aerodyne Research Inc.; Lee et al., 2014) and two proton-transfer reaction mass-spectrometry (PTR-MS) instruments: Vocus-2R-PTR-TOF (TOFWERK A.G.; Krechmer et al., 2018) and PTR3 (Ionicon Analytik; Breitenlechner et al., 2017). The latter instrument was operated in a switching-mode regime using $H_3O^+(H_2O)_n$, n=0-1 (as H_3O^+-CIMS) and $NH_4^+(H_2O)_n$, n = 0-2 (as NH_4^+-CIMS) primary ions (Hansel et al., 2018; Zaytsev et al., 2019). Switching between ion modes occurred every five minutes.~~ Aromatic precursors as well as gas-phase oxygenated volatile organic compounds (OVOCs) were detected

by chemical ionization high-resolution time-of-flight mass spectrometry (CIMS) techniques: I^- CIMS, NH_4^+ CIMS, and H_3O^+ CIMS. The I^- CIMS instrument (Aerodyne Research Inc.) is described by Lee et al. (2014). NH_4^+ CIMS and H_3O^+ CIMS were carried out using a mass spectrometer (PTR3, Ionicon Analytik) which was operated in two ionization modes: $H_3O^+ \cdot (H_2O)_n$, n=0-1 (as PTR3 H_3O^+ CIMS, Breitenlechner et al., 2017) and $NH_4^+ \cdot (H_2O)_n$, n=0-2 (as PTR3 NH_4^+ CIMS, Zaytsev et al., 2019). Switching between ion modes occurred every five minutes. H_3O^+ CIMS was also conducted by a proton-transfer-reaction mass spectrometer (Vocus-2R-PTR, Aerodyne Research Inc.; Krechmer et al., 2018).

30. What reagent gas was used for the Vocus-2R-PTR?

Vocus-2R-PTR uses hydronium (H_3O^+) ions to ionize VOCs (Krechmer et al., 2018).

31. The authors should provide the 10 compounds used in the calibration of I^-CIMS and PTR3 in SI. Using these instruments for aerosol characterization may be associated with sampling artefacts as discussed recently (see my general comments)

We include the following tables containing calibrated species and measured sensitivities in the SI:

Table S2: Sensitivities of I^- CIMS for calibrated species.

Species	*Ion formula*	*m/z*	*Sensitivity (ndcps/ppb)*
Formic acid	$CH_2O_2I^-$	*172.91*	*3000*
Acetic acid	$C_2H_4O_2I^-$	*186.93*	*130*
Acrylic acid	$C_3H_4O_2I^-$	*198.93*	*63*
Glycolic acid	$C_2H_4O_3I^-$	*202.92*	*880*
cis-2-butene-1,4-diol	$C_4H_8O_2I^-$	*214.96*	*1600*
1,2-butanediol	$C_4H_{10}O_2I^-$	*216.97*	*110*
Phenol	$C_6H_6OI^-$	*220.95*	*180*
Malonic acid	$C_3H_4O_4I^-$	*230.92*	*74*
o-cresol	$C_7H_8OI^-$	*234.96*	*65*
Nitrophenol	$C_6H_5NO_3I^-$	*265.93*	*38500*

Table S3: Sensitivities of PTR3 H_3O^+ CIMS and PTR3 NH_4^+ CIMS for calibrated species.

Species	*PTR3 H_3O^+ CIMS*			*PTR3 NH_4^+ CIMS*		
	Ion formula	*m/z*	*Sensitivity (ndcps/ppb)*	*Ion formula*	*m/z*	*Sensitivity (ndcps/ppb)*
Acetone	$C_3H_6OH^+$	*59.05*	*12900*	$C_3H_6ONH_4^+$	*76.08*	*10600*
Acetic acid	$C_2H_4O_2H^+$	*61.03*	*9600*	$C_2H_4O_2NH_4^+$	*78.06*	*840*
Methacrolein	$C_4H_6OH^+$	*71.05*	*15300*	$C_4H_6ONH_4^+$	*88.08*	*4900*
2-furanone	$C_4H_4O_2H^+$	*85.03*	*20700*	$C_4H_4O_2NH_4^+$	*102.06*	*10300*
Diacetyl	$C_4H_6O_2H^+$	*87.04*	*5000*	$C_4H_6O_2NH_4^+$	*104.07*	*5200*
Angelica lactone	$C_5H_6O_2H^+$	*99.04*	*19400*	$C_5H_6O_2NH_4^+$	*116.07*	*20800*
Benzaldehyde	$C_7H_6OH^+$	*107.05*	*16200*	$C_7H_6ONH_4^+$	*124.07*	*14500*
o-cresol	$C_7H_8OH^+$	*109.07*	*6900*	$C_7H_8ONH_4^+$	*126.09*	*370*
1,2,4-TMB	$C_9H_{12}H^+$	*121.10*	*1640*	$C_9H_{12}NH_4^+$	*138.13*	*800*
3-decanone	$C_{10}H_{20}OH^+$	*157.16*	*13600*	$C_{10}H_{20}ONH_4^+$	*174.19*	*23200*

32. Page 5, lines 4-24. Please provide time series for $[ArVOC]_0$ for toluene and 124-TMB as I suggested before? Data obtained from PTR!

Time series of toluene and 1,2,4-TMB levels measured by Vocus-2R-PTR and dilution-corrected concentrations are shown in Fig. R6.

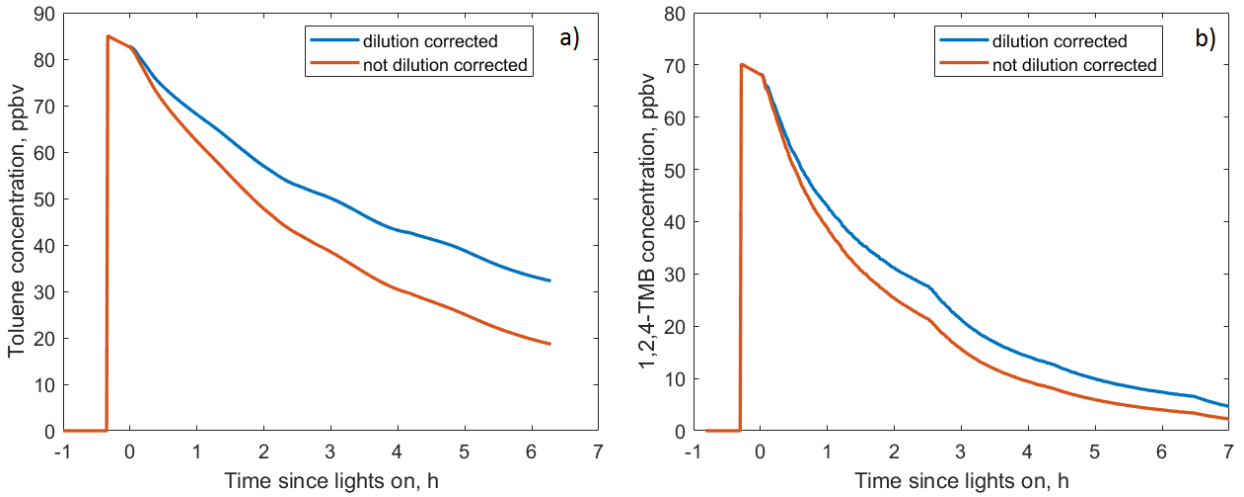

Figure R6: Dilution corrected and not dilution corrected concentrations of (a) toluene and (b) 1,2,4-TMB in photooxidation experiments.

33. Page 5. The yields were described but were not provided in the paper!

The yields of major first-generation oxidation products for both toluene and 1,2,4-TMB oxidation experiments are given in Tables 1 and 2.

34. What "b" represents in eq. 3?

Parameter *b* is the offset. Since it does not have any chemical sense, we leave it out of the equation:

$$[X]^{corr} = Y[ArVOC]^{reacted} \sout{+ b} \quad (3)$$

35. Page 4, line 31. Is the light intensity was measured?

The spectrum of the chamber lights was measured, while the total light intensity is unknown. Hence, the chamber light intensity in the model was tuned to match the measured time-dependent concentrations of aromatic compounds with the modelled values (P4 L31).

36. Page 4, 5: Gamma Kinetic parameterization. Can the structure affect the results (the parameters obtained)? This model is applied to formulas here?

GKP was applied to the oxidation products observed in this study. The generation parameter *m* and kinetic parameter *k* for a given species depend on the number of reactions with OH needed to produce that species and the effective second-order rate constant, respectively. Therefore, compounds with different structures will likely have different parameters *m* and *k*. However, CIMS and PTR-MS instruments cannot distinguish between isomers and do not provide further insight into the molecular structure of detected compounds. Hence, it is possible that several compounds with the same molecular formulas, but different

structures were lumped together and returned a non-integer parameter *m*. The generation parameter *m* and kinetic parameter *k* for major oxidation products are given in Tables 1 and 2.

37. Page 6, line 18. Figure 1 should incorporate both HCs as I stated before.

We include Figure 1 in this paper to illustrate four major oxidation pathways common for numerous aromatic compounds (including toluene and 1,2,4-TMB). Hence, we think it would be overwhelming to add 1,2,4-TMB oxidation scheme to this figure as toluene and 1,2,4-TMB schemes are quite similar. However, in response to this comment we modify the following sentence (P6 L17):

~~*The toluene oxidation scheme from MCM v3.3.1 is shown on Fig. 1.*~~ *These four channels are illustrated using the example of toluene in Fig. 1.*

38. Page 10, line 18. Define TD-NH_4^+ CIMS.

The definition of TD-NH_4^+ CIMS was given on page 4, line 24 (NH_4^+ CIMS instrument equipped with thermal denuder).

39. Figure 6. Figure 6 title. I think there is an error! (a) should be toluene and (b) should be 124-TMB. Please clarify? Also is total organics or total organics carbon?

We thank the reviewer for spotting this typo and update the title as suggested:

Figure 6: Total organics measured in the particle phase by NH_4^+ CIMS and binned by the carbon atom number (a) in the toluene ~~1,2,4-TMB~~ photooxidation experiment and (b) the 1,2,4-TMB ~~toluene~~ photooxidation experiment. Total carbon measured by AMS is in red.

40. Page 10. "The O:C ratios calculated from individual species measured from thermally desorbed SOA using NH_4^+ CIMS were ~0.95 for toluene SOA and ~0.7 for 1,2,4-TMB SOA. These ratios are in good agreement with the atomic O:C ratios measured by AMS (0.85 and 0.65 for toluene and 1,2,4-TMB SOA, respectively) (Canagaratna et al., 2015)." Does this comparison was applied to the same SOA size for the AMS and CIMS?

AMS transmission efficiency is maximum (100%) for particles with diameters from 100 nm to 550 nm (Knote et al., 2015). PTR3 instrument used for the particle-phase measurements was equipped with a gas-phase denuder (Ionicon Analytic GmbH, Austria) that removes the gas-phase organics. Particles smaller than 100 nm in diameter do not pass through a denuder and are not analysed in the instrument (Eichler et al., 2015). Hence, the AMS and CIMS instruments were used to analyze the composition of aerosols of the same size.

41. Page 10. "Products observed in the gas phase are compared to those detected in the particle phase to further understand the mechanism of SOA formation from aromatics precursors." Can partitioning coefficients be obtained for these products? Please provide organic species present in both gas phase and particle phase and their estimated partitioning coefficient? Table for example.

Partitioning coefficients for low-volatile compounds could be obtained if the equilibrium between the gas and particle-phase organics was achieved. However, there are a number of reasons why simple gas-particle partitioning might not explain the concentrations observed in the two phases. First, chamber lights were turned on during the whole duration of experiments resulting in constant production and loss of oxidation products in the gas phase. Second, particles were lost on the chamber walls, while the wall

loss term was not estimated. Third, CIMS and PTR-MS instruments cannot distinguish between isomers and do not provide further insight into the molecular structure of detected compounds. Hence, it is possible that several compounds with the same molecular formulas, but different structures and partitioning coefficients were lumped together. Therefore, partitioning coefficients for observed species cannot be reported.

42. The section describing on page 10, lines 25 - 32. "non-fragmentary" "ring-retaining" "ring scission" "fragmentary" is not clear to me. Could the authors describe how the thermal fragmentation either in the gas phase or the particle phase reported on page 10 can affect the data (formula and structures) provided in this manuscript? Are the HOMs detected not originated from artefacts in the inlets? These compounds with high O:C ratio are expected to be in the particle phase but numerous studies including this one report them in the gas phase?

During particle-phase measurements, sampled air passes through a gas-phase denuder (Ionicon Analytik GmbH, Austria) that removes the gas-phase organics and then through a thermal desorption region heated to 180℃ that vaporizes the aerosol particles. This may result in thermal decomposition of OVOCs. We studied thermal decomposition of OVOCs extracted from alpha-pinene SOA by measuring their peak intensities using TD-NH_4^+ CIMS. Signals of many species increased at moderate temperatures (T < 160℃) and levelled out or decreased at higher temperatures (T > 180℃), as shown in Fig. R1 (Zaytsev et al., 2019). Therefore, we chose the TDU temperature to be 180℃, as at this temperature the major fraction of particles was evaporated while thermal decomposition of labile species was relatively small.

We modify the description of TD-NH_4^+ CIMS and TD-H_3O^+ CIMS (P4 L21):

Particle-phase compounds were quantified using the FIGAERO-HRToF-I^- CIMS (Lopez-Hilfiker et al., 2014), and a second PTR3 that could be operated in two positive modes as described above and equipped with an aerosol inlet comprising a gas-phase denuder and a thermal desorption unit heated to 180℃ (TD-NH_4^+ CIMS and TD-H_3O^+ CIMS). At this temperature, all particles were evaporated while thermal decomposition of labile oxygenated compounds was relatively small (Zaytsev et al., 2019).

Low volatile organic compounds (LVOC) including HOMs have low saturation vapour pressure such that almost every collision with wall inlet leads to a complete loss. However, the estimates for these losses in the literature have shown significant discrepancy. Breitenlechner et al. (2017) estimated the wall losses for LVOC with more than five oxygens in the PTR3 inlet to be 80% while for VOC with less than five oxygens the wall losses were assumed to be negligible. Hansel et al. (2018) evaluated the wall losses in the CI3-ToF inlet to be 50%. Since we did not have an additional instrument with calibrated diffusion losses in the inlet (i.e., acetate CIMS), we did not take into account wall losses of less volatile species in inlets of used instrumentation. It results in underestimation of the yield of these compounds including HOMs.

In order to avoid potential ambiguity, we replace the term "non-fragmentary" by "non-fragmented" throughout the manuscript.

43. In general, chamber backgrounds NO_x always is present (although clean air was used) due to wall chemistry and the history of the chamber (heterogeneous wall chemistry). Comments!

Between experiments, the environmental chamber was cleaned by flushing with purified air for at least 10 hours while the chamber lights were turned on. As a result, NO_x background levels before experiments

were less than 5 ppbv (Fig. S1). However, HONO+NO_x levels during experiments were much higher (~30 ppbv, Fig. S1).

References:

Breitenlechner, M., Fischer, M., Hainer, M., Heinritzi, M., Curtius, M., and Hansel, A.: PTR3: An instrument for Studying the Lifecycle of Reactive Organic Carbon in the Atmosphere, Anal. Chem., 89, 5824–5831, https://doi.org/10.1021/acs.analchem.6b05110, 2017.

Buhr, K., van Ruth, S., and Delahunty, C.: Analysis of volatile flavour compounds by Proton Transfer Reaction-Mass Spectrometry: fragmentation patterns and discrimination between isobaric and isomeric compounds, Int. J. Mass Spectrom., 221, 1–7, https://doi.org/10.1016/S1387-3806(02)00896-5, 2002.

Calvert, J., Atkinson, R., Becker, K.H., Kamens, R., Seinfeld, J., Wallington, T., and Yarwood, G.: The mechanisms of atmospheric oxidation of aromatic hydrocarbons, Oxford University Press, Inc., New York, 2002.

Eichler, P., Müller, M., D'Anna, B., and Wisthaler, A.: A novel inlet system for online chemical analysis of semi-volatile submicron particulate matter, Atmos. Meas. Tech., 8, 1353–1360, https://doi.org/10.5194/amt-8-1353-2015, 2015.

Erickson, M. H., Gueneron, M., and Jobson, B. T.: Measuring long chain alkanes in diesel engine exhaust by thermal desorption PTR-MS, Atmos. Meas. Tech., 7, 225–239, https://doi.org/10.5194/amt-7-225-2014, 2014.

Hansel, A., Scholz, W., Mentler, B., Fischer L., and Berndt, T.: Detection of RO2 radicals and other products from cyclohexene ozonolysis with NH4+ and acetate ionization mass spectrometry, Atmos. Env., 186, 248–255, doi:10.1016/j.atmosenv.2018.04.023, 2018.

Hazenkamp-von Arx, M.E., Gotschi, T., Ackermann-Liebrich, U., Bono, R., Burney, P., Cyrys, J., Jarvis, D., Lillienberg, L., Luczynska, C., Maldonado J.A., Jaen, A., de Marco, R., Mi, Y., Modig L., Bayer-Oglesby, L., Payo, F., Soon, A., Sunyer, J., Villani, S., Weyler, J., and Kunzli N.: $PM_{2.5}$ and NO_2 assessment in 21 European study centres of ECRHS II: annual means and seasonal differences, Atmos. Env., 38, 1943–1953, https://doi.org/10.1016/j.atmosenv.2004.01.016, 2004.

Jang, M., and Kamens, R.M.: Characterization of Secondary Aerosol from the Photooxidation of Toluene in the Presence of NO_x and 1-Propene, Environ. Sci. Technol., 35, 3626-3639, https://doi.org/10.1021/es010676+, 2001.

Kleindienst, T.E., Conver, T.S., McIver, C.D., and Edney, E.O.: Determination of Secondary Organic Aerosol Products from the Photooxidation of Toluene and their Implications in Ambient $PM_{2.5}$, Journal of Atmospheric Chemistry, 47, 79-100, https://doi.org/10.1023/B:JOCH.0000012305.94498.28, 2004.

Knote, C., Brunner, D., Vogel, H., Allan, J., Asmi, A., Äijälä, M., Carbone, S., van der Gon, H. D., Jimenez, J. L., Kiendler-Scharr, A., Mohr, C., Poulain, L., Prévôt, A. S. H., Swietlicki, E., and Vogel, B.: Towards an online-coupled chemistry-climate model: evaluation of trace gases and aerosols in COSMO-ART, Geosci. Model Dev., 4, 1077–1102, https://doi.org/10.5194/gmd-4-1077-2011, 2011.

Krechmer, J.E., Lopez-Hilfiker, F., Koss, A., Hutterli, M., Stoermer, C., Deming, B., Kimmel, J., Warneke, C., Holzinger, R., Jayne, J., Worsnop, D., Fuhrer, K., Gonin, M., and de Gouw J.: Evaluation of a New Vocus

Reagent-Ion Source and Focusing Ion-Molecule Reactor for use in Proton-Transfer-Reaction Mass Spectrometry, Anal. Chem., 90, 20, 12011-12018, doi:10.1021/acs.analchem.8b02641, 2018.

Li, Z., Smith, K. A., and Cappa, C. D.: Influence of relative humidity on the heterogeneous oxidation of secondary organic aerosol, Atmos. Chem. Phys., 18, 14585–14608, https://doi.org/10.5194/acp-18-14585-2018, 2018.

Pagonis, D., Krechmer, J. E., de Gouw, J., Jimenez, J. L., and Ziemann, P. J.: Effects of gas–wall partitioning in Teflon tubing and instrumentation on time-resolved measurements of gas-phase organic compounds, Atmos. Meas. Tech., 10, 4687–4696, https://doi.org/10.5194/amt-10-4687-2017, 2017.

Saukko, E., Lambe, A. T., Massoli, P., Koop, T., Wright, J. P., Croasdale, D. R., Pedernera, D. A., Onasch, T. B., Laaksonen, A., Davidovits, P., Worsnop, D. R., and Virtanen, A.: Humidity-dependent phase state of SOA particles from biogenic and anthropogenic precursors, Atmos. Chem. Phys., 12, 7517-7529, https://doi.org/10.5194/acp-12-7517-2012, 2012.

Seinfeld, J.H., and Pandis, S.N.: Atmospheric Chemistry and Physics: From Air Pollution to Climate Change, Wiley, Hoboken NJ, 2016.

Yuan, B., Koss, A.R., Warneke, C., Coggon, M., Sekimoto, K., and de Gouw, J.A.: Proton-Transfer-Reaction Mass Spectrometry: Applications in Atmospheric Sciences, Chem. Rev., 117, 13187-13229, https://doi.org/10.1021/acs.chemrev.7b00325, 2017.

Wu, R., Pan, S., Li, Y., and Wang, L.: Atmospheric Oxidation Mechanism of Toluene, J. Phys. Chem. A., 118, 4533-4547, https://doi.org/10.1021/jp500077f, 2014.

Zaytsev, A., Breitenlechner, M., Koss, A. R., Lim, C. Y., Rowe, J. C., Kroll, J. H., and Keutsch, F. N.: Using collision-induced dissociation to constrain sensitivity of ammonia chemical ionization mass spectrometry (NH4+ CIMS) to oxygenated volatile organic compounds, Atmos. Meas. Tech., 12, 1861–1870, https://doi.org/10.5194/amt-12-1861-2019, 2019.

Response to Reviewer 2

Reviewer comments are in **bold**. Author responses are in plain text. Excerpts from the manuscript are in *italics*. Modifications to the manuscript are in *blue italics*. Page and line numbers in the responses correspond to those in the original ACPD paper.

In this work, the authors presented results from oxidation experiments of aromatic compounds, toluene and 1,2,4-TMB. These aromatic compounds are important VOCs in urban areas, and their oxidation leads to significant ozone and secondary organic aerosol (SOA) formation. In this study the authors employed a number of new analytical techniques to measure the gas and particle phase composition, and compared to the latest version of Master Chemical Mechanism (MCM), which summarizes the current understanding about the mechanisms. Furthermore, the time trend analysis using gamma kinetic parameterization is a novel method to look at the multigenerational chemistry. This manuscript is well written, and I only have some minor suggestions. I recommend publication of this manuscript in ACP.

We would like to thank the reviewer for the positive reception of our work and constructive comments that helped us to improve our manuscript. In this document we provide our replies to the reviewer's comments.

1. It would be good to know on a bulk or general level, how these results improve the understanding of the chemistry. For example, I wonder what the carbon closure now is, with these new measurements. Figure 3 is probably a good place to show that.

The objective of this study is to evaluate the importance of various gas-phase oxidation pathways of aromatic compounds in terms of production of oxygenated low-volatile species (including HOMs) and SOA formation potential (P3 L5). Bulk organic carbon properties such as volatility, oxidation state, and reactivity, as well as carbon closure will be discussed in an accompanying paper currently under preparation.

2. Somewhat related: One key piece of information shown in Section 3.3 and Fig. 6 is that the total SOA mass measured by AMS and NH_4^+ CIMS compare very well, and so do the O/C ratios. This is an important discovery and should be highlighted in the abstract.

We agree with the reviewer that this is an important discovery. We underline this finding in Conclusions (P11 L28):

Many of these compounds are low in volatility and comprise a significant fraction (more than 25%) of SOA mass, which was measured using AMS and TD-NH_4^+ CIMS and the two measurements are in good agreement.

3. The multigenerational chemistry of many of the products is a key contribution. I expect that the accompanying paper describing the methods will be well received. There are some ambiguous ones that have non-integer m (e.g. 1.7-1.8). What is the general uncertainty in this analysis?

Noise can contribute to uncertainty in returned values of *m*. At low generations (*m*=1-2), the standard deviation of the fit is 0.1, while it can be higher (up to 0.8) at higher (3+) generations. Hence, it is possible

that the compounds with non-integer *m* are produced by more than one pathway with different number of reaction steps.

We add the following sentence to the manuscript (P6 L13):

At low generations (m=1-2), the standard deviation of the fit is 0.1, while it can be higher (up to 0.8) at higher (3+) generations (Koss et al., 2019).

4. Related to comment/question 3: I expect that some experiments with oxidation of later generation products would be very helpful. For example, oxidation of cresol (which is commercially available) should yield lower m for some of the products. Perhaps even examining the decrease in m would help apportion the relative amount for each generation. I think these are important experiments anyway given that the authors are claiming the importance of phenolic and benzaldehyde pathways in HOM production.

We agree with the reviewer that experiments with oxidation of later generation products (e.g., cresols and benzaldehydes) would be very helpful to further investigate different pathways in which highly oxygenated compounds are produced. While we plan to conduct these experiments in the future, we think that they are out of the scope of the current work.

5. The experiments were all conducted under RH of 2%. While I completely understand the rationale to create a well-controlled environment, it may be worthwhile to mention this is a potential limitation of this study and discuss implications. I do not see water playing an important role in the gas-phase chemistry, but could potentially shorten the lifetime of particle-phase hydroperoxides, epoxides and organic nitrates.

We add the following sentence as suggested (P3 L12):

The temperature of the chamber was controlled at 292 (+/- 1) K ~~and approximately 2% relative humidity~~. All experiments were carried out under dry conditions (relative humidity, RH ≅2%, +/- 1%) to simplify gas- and particle-phase measurements. Higher RH can potentially shorten the lifetime of particle-phase hydroperoxides, epoxides and organonitrates (Li et al., 2018) as well as affect gas-particle partitioning kinetics and thermodynamics (Saukko et al., 2012).

Methods: I do not understand why the authors would use hexafluorobenzene as a tracer for both chamber wall loss and dilution of VOCs. I can see hexafluorobenzene is a good tracer for dilution, but I do not expect it to be lost to the chamber walls. Based on the chamber volume and air refilling rate, the dilution rate can be estimated. Is the hexafluorobenzene decaying faster than this dilution rate? If so, why is it being lost to the walls?

We used hexafluorobenzene as a tracer for the dilution of VOCs, not as a tracer for vapour-phase wall loss. The reviewer is correct that a highly volatile compound like hexafluorobenzene is not expected to be lost to the chamber walls. The hexafluorobenzene loss rate was consistent with the known chamber volume and dilution air flow. Vapour wall loss was quantified using the "rapid burst" method (Krechmer et al., 2016), and the rate constant of this process $k_{\text{wall loss}}$ was estimated to be $5 \cdot 10^{-4}$ s^{-1}.

To make this point clearer, we edit the following sentences:

P4 L32: *The ~~chamber wall loss and~~ dilution term for volatile compounds was estimated based on the concentration of the dilution tracer, hexafluorobenzene.*

P5 L4: *The OH concentration was determined using the decay of the aromatic precursor, accounting for losses from dilution ~~and chamber wall deposition~~.*

We also update equation 1:

$$[\mathrm{ArVOC}]_t = [\mathrm{ArVOC}]_0 \cdot \exp\left(-k_{\mathrm{ArVOC+OH}} \cdot [\mathrm{OH}_{\mathrm{exposure}}]_t - k_{\text{~~physical loss ArVOC~~ dilution}} \cdot t\right) \qquad (1)$$

CO and formaldehyde were mentioned in methods, but no results were presented.

CO and formaldehyde will be discussed in further details in the accompanying paper under preparation. Since they play no role in the present paper, we remove the sentence describing CO and formaldehyde measurements from the manuscript (P4 L17).

Methods: Particle-phase compounds were quantified using I^- CIMS, but for the gas phase compounds the authors claim I^- CIMS is quite uncertain. Are the uncertainties in quantification the same for both phases?

Particle-phase compounds were quantified using both the FIGAERO-HRToF-I^--CIMS and a second PTR3 equipped with an aerosol inlet comprising a gas-phase denuder and a thermal desorption unit (TD-NH_4^+ CIMS). Total organic mass and O:C ratio measured by TD-NH_4^+ CIMS are in good agreement with the AMS measurements (P10 L21). As for FIGAERO-HRToF-I^--CIMS, uncertainties of the particle-phase measurements are similar to the gas-phase measurements.

We add the following clarification to the manuscript (P4 L24):

Uncertainties of the particle-phase CIMS measurements are similar to the corresponding uncertainties of the gas-phase CIMS instruments.

Section 2.4: how large are the time steps?

The time step Δt was five minutes which corresponds to the switching period between two ionization modes of PTR3 (P4 L5).

Section 3.1: Is it possible that the epoxide was not detected because of thermal decomposition for the particle phase measurements, or fragmentation during ionization?

The reviewer raises an interesting point. While it is possible that the epoxide was decomposed or fragmented during ionization, we think that it should have been detected using the instrumentation implemented in this study. We calibrated PTR3 NH_4^+ CIMS and H_3O^+ CIMS for isoprene epoxydiol (trans-IEPOX) and observed very little fragmentation in NH_4^+ CIMS comparing to H_3O^+ CIMS (Fig. R1).

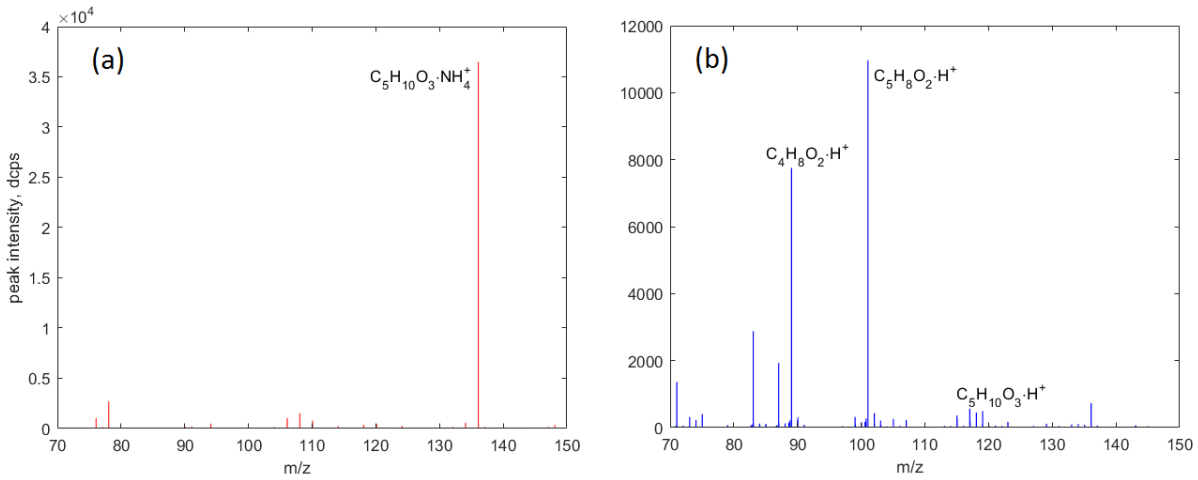

Figure R1: High-resolution mass-spectra obtained during calibration of trans-IEPOX in (a) PTR3 NH_4^+ CIMS and (b) PTR3 H_3O^+ CIMS.

In addition, we studied thermal decomposition of OVOCs extracted from alpha-pinene SOA by measuring their peak intensities using TD-NH_4^+ CIMS. Signals of many species increased at moderate temperatures (T<160°C) and levelled out or decreased at higher temperatures (T>180°C), as shown in Fig. R2. Therefore, we chose the TDU temperature to be 180°C, as at this temperature all particles were evaporated while thermal decomposition of labile species was relatively small.

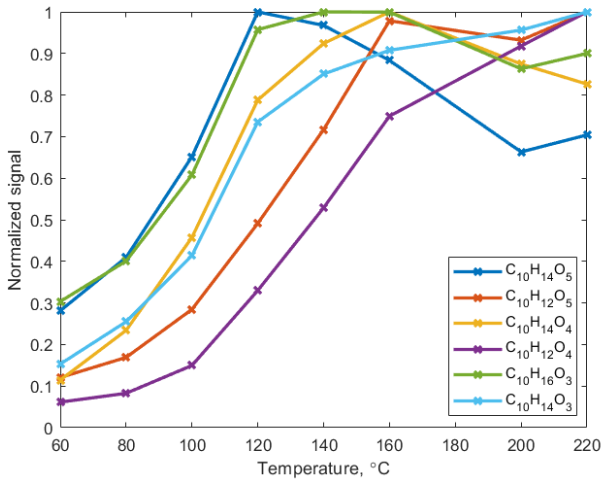

Figure R2: Thermograms of select OVOCs extracted from alpha-pinene ozonolysis SOA.

Hence, we think that toluene and 1,2,4-TMB epoxides should be detectable using NH_4^+ CIMS.

Section 3.2.1, Line 13: BPR has been defined earlier.

We thank the reviewer for spotting this typo in the manuscript and remove the abbreviation ("BPR") from the manuscript (P7 L13).

Section 3.2.1 Line 29-30: Presumably the lifetimes are calculated using generic RO_2+NO and RO_2+HO_2 rate constants? What rate constants were used?

The rate constants were estimated using information from MCM v3.3.1.
For toluene:
$k_{\mathrm{RO_2+HO_2}} = 2.05 \cdot 10^{-11}$ cm^3 molecule^{-1} s^{-1}, $k_{\mathrm{RO_2+NO}} = 9.26 \cdot 10^{-12}$ cm^3 molecule^{-1} s^{-1}.
For 1,2,4-TMB:
$k_{\mathrm{RO_2+HO_2}} = 2.22 \cdot 10^{-11}$ cm^3 molecule^{-1} s^{-1}, $k_{\mathrm{RO_2+NO}} = 9.26 \cdot 10^{-12}$ cm^3 molecule^{-1} s^{-1}.

Tables 1-3: what are the uncertainties in m from the fits?

Noise can contribute to uncertainty in returned values of *m*.

We add the following sentence to the manuscript (P6 L13):

At low generations (m=1-2), the standard deviation of the fit is 0.1, while it can be higher (up to 0.8) at higher (3+) generations (Koss et al., 2019).

Figure 6: why is there a discontinuity at 14 hours of exposure for toluene? Was more OH precursor added? Similarly there seems to be one as well for TMB at 4 h.

During experiments, additional injections of HONO were added to the chamber to roughly maintain the OH levels (Fig. S1). Discontinuities in particle-phase signals are indeed caused by the additional HONO injections.

References

Krechmer, J.E., Pagonis, D., Ziemann, P.J., and Jimenez, J.L.: Quantification of Gas-Wall Partitioning in Teflon Environmental Chambers Using Rapid Bursts of Low-Volatility Oxidized Species Generated in Situ, Environ. Sci. Technol. 50(11), 5757−5765, https://doi.org/10.1021/acs.est.6b00606, 2016.

Li, Z., Smith, K. A., and Cappa, C. D.: Influence of relative humidity on the heterogeneous oxidation of secondary organic aerosol, Atmos. Chem. Phys., 18, 14585–14608, https://doi.org/10.5194/acp-18-14585-2018, 2018.

Saukko, E., Lambe, A. T., Massoli, P., Koop, T., Wright, J. P., Croasdale, D. R., Pedernera, D. A., Onasch, T. B., Laaksonen, A., Davidovits, P., Worsnop, D. R., and Virtanen, A.: Humidity-dependent phase state of SOA particles from biogenic and anthropogenic precursors, Atmos. Chem. Phys., 12, 7517-7529, https://doi.org/10.5194/acp-12-7517-2012, 2012.

Mechanistic Study of Formation of Ring-retaining and Ring-opening Products from Oxidation of Aromatic Compounds under Urban Atmospheric Conditions

Alexander Zaytsev[1], Abigail R. Koss[2], Martin Breitenlechner[1], Jordan E. Krechmer[3], Kevin J. Nihill[2], Christopher Y. Lim[2], James C. Rowe[2], Joshua L. Cox[4], Joshua Moss[2], Joseph R. Roscioli[3], Manjula R. Canagaratna[3], Douglas R. Worsnop[3], Jesse H. Kroll[2], and Frank N. Keutsch[1,4,5]

[1]John A. Paulson School of Engineering and Applied Sciences, Harvard University, Cambridge, MA 02138, USA,
[2]Department of Civil and Environmental Engineering, Massachusetts Institute of Technology, Cambridge, MA 02139, USA,
[3]Aerodyne Research Inc., Billerica, MA 01821, USA,
[4]Department of Chemistry and Chemical Biology, Harvard University, Cambridge, MA 02138, USA,
[5]Department of Earth and Planetary Sciences, Harvard University, Cambridge, MA 02138, USA

Correspondence to: Alexander Zaytsev (zaytsev@g.harvard.edu) and Frank N. Keutsch (keutsch@seas.harvard.edu)

Abstract. Aromatic hydrocarbons make up a large fraction of anthropogenic volatile organic compounds and contribute significantly to the production of tropospheric ozone and secondary organic aerosol (SOA). Four ~~A series of~~ toluene and four 1,2,4-trimethylbenzene (1,2,4-TMB) photooxidation experiments were performed in an environmental chamber under relevant polluted conditions (NO_x ~ 10 ppb). An extensive suite of instrumentation including two Proton-Transfer Reaction Mass-Spectrometers (PTR-MS) and two Chemical Ionization Mass-Spectrometers (NH_4^+ CIMS and I^- CIMS) allowed for quantification of reactive carbon in multiple generations of hydroxyl radical (OH)-initiated oxidation. ~~Hydroxyl radical (OH)-initiated~~ Oxidation of both species produces ring-retaining products such as cresols, benzaldehydes, and bicyclic intermediate compounds, as well as ring scission products such as epoxides, and dicarbonyls. We show that the oxidation of bicyclic intermediate products leads to formation of compounds with high oxygen content (O:C ratio up to 1.1). These compounds, previously identified as highly oxygenated molecules (HOMs), are produced by more than one pathway with differing numbers of reaction steps with OH, including both autooxidation and phenolic pathways. We report the elemental composition of these compounds formed under relevant urban high-NO conditions. We show that ring-retaining products for these two precursors are more diverse and abundant than predicted by current mechanisms. We present speciated elemental composition of SOA for both precursors and confirm that highly oxygenated products make up a significant fraction of SOA. Ring scission products are also detected in both the gas and particle phases, and their yields and speciation overall agree with the kinetic model prediction.

1 Introduction

Aromatic compounds represent a significant fraction of volatile organic compounds (VOCs) in the urban atmosphere and play a substantial role in the formation of tropospheric ozone and secondary organic aerosol (SOA) (Calvert et al., 2002). Typical anthropogenic sources include vehicle exhaust, solvent use, and evaporation of gasoline and diesel fuels. Toluene, the most abundant alkylbenzene in the atmosphere, is primarily emitted by aforementioned anthropogenic processes (Wu et al., 2014). Toluene-derived SOA is estimated to contribute approximately 17-29% of the total SOA produced in urban areas (Hu et al., 2008). More highly substituted aromatic compounds make up another important group of aromatic compounds as they tend to have high SOA yields (Li et al., 2016) and account for a significant fraction of non-methane hydrocarbons in the industrialized regions of China (Tang et al., 2007; Zheng et al., 2009). 1,2,4-trimethylbenzene (1,2,4-TMB) is chosen ~~serves~~ as a model molecule to study oxidation of more substituted aromatic compounds (i.e., trimethylbenzenes).

In the atmosphere, oxidation of aromatic hydrocarbons is primarily ~~most often~~ initiated by their reactions with hydroxyl radicals (OH) via H-abstraction from the alkyl groups or OH addition to the aromatic ring (Fig. 1) (Calvert et al., 2002). The abstraction channels are relatively minor, leading to the formation of benzyl radicals and benzaldehyde with yields of ~0.07 in the case of toluene (Wu et al., 2014) and ~0.06 in the case of 1,2,4-TMB (Li and Wang, 2014). The OH-adducts can react with atmospheric O_2 through H-abstraction to form ring-retaining phenolic compounds (i.e., cresols and trimethylphenols) (Jang and Kamens, 2001; Kleindienst et al., 2004). The phenol formation yield decreases for the more substituted aromatics: in case of toluene the cresol yield is ~0.18 (Klotz et al., 1998, Smith et al., 1998) while for 1,2,4-TMB the trimethylphenol yield is ~0.03 (Bloss et al., 2005). Both abstraction and phenolic channels lead to the formation of products retaining the aromatic ring. The OH-adducts can also react with O_2 through recombination. In this case they lose aromaticity and form non-aromatic ring-retaining bicyclic peroxy radicals (BPRs). Under urban-relevant high-NO conditions BPRs also react with NO to form bicyclic oxy radicals that decompose to ring scission carbonylic products such as (methyl) glyoxal and biacetyl. Recent theoretical studies predict a new type of epoxy-dicarbonyl products that have not reported in previous studies (Li and Wang, 2014, Wu et al., 2014). Reaction of BPRs with NO can also result in formation of bicyclic organonitrates. In addition, ~~Under low-NO conditions,~~ BPRs react with HO_2 and RO_2, forming bicyclic hydroperoxides and bicyclic carbonyls, respectively (Fig. 2). Finally, ~~In addition,~~ BPRs can undergo unimolecular H-migration followed by O_2-addition (~~so-called~~ autooxidation) leading to the formation of non-aromatic ring-retaining highly oxygenated organic molecules (HOMs) (Bianchi et al., 2019). Molteni et al. (2018) reported elemental composition of the HOMs from a series of aromatic compounds produced under low-NO conditions. The autooxidation pathway might be more important for the substituted aromatics because of the higher yield of BPR formation and the larger number of relatively weak C-H bonds (Wang et al., 2017). ~~Under urban-relevant high-NO conditions BPRs also react with NO to form bicyclic oxy radicals that decompose to ring scission carbonylic products such as (methyl) glyoxal and biacetyl. Recent theoretical studies predict a new type of epoxy-dicarbonyl products that have not reported in previous studies (Li and Wang, 2014, Wu et al., 2014). Reaction of BPRs with NO can also result in formation of bicyclic organonitrates.~~ Both ring-retaining and ring scission compounds are expected to be low in volatility and contribute

significantly to SOA (Schwantes et al., 2017). There remain a number of major uncertainties in model representation of oxidation of aromatic compounds including overprediction of ozone concentration, underprediction of OH production and lack of detailed description of SOA formation (Birdsall and Elrod, 2011; Wyche et al., 2009).

In the present work, we investigate ~~the~~ detailed mechanisms of hydroxyl radical multigeneration oxidation chemistry of two aromatic hydrocarbons: toluene and 1,2,4-trimethylbenzene under moderately high ~~moderate~~, urban-relevant NO_x levels (~10 ppbv). Laboratory experiments were conducted at an environmental chamber over approximately 1 day of atmospheric-equivalent oxidation. ~~We use four high-resolution time-of-flight chemical ionization mass spectrometers (NH_4^+ CIMS, I^- CIMS and two PTR-MS) to characterize and quantify gas- and particle-phase oxidation products.~~ We use three chemical ionization mass spectrometry (CIMS) techniques (I^- reagent ion, NH_4^+ reagent ion, and H_3O^+ reagent ion) to characterize and quantify gas-phase oxidation products. In addition, NH_4^+ CIMS and I^- CIMS were used to detect particle-phase products. The goal of this work is to ~~We~~ identify gas-phase pathways leading to production of low-volatility compounds which are important for SOA formation and support these identifications with CIMS data and a method to characterize the kinetics of an oxidation system.

2 Methods

2.1 Experimental design

All experiments were performed in a 7.5 m^3 Teflon environmental chamber (Hunter et al., 2014). Prior to experiments, the chamber was flushed and filled with purified air. During experiments the environmental chamber was operated in the constant-volume ("semi-batch") mode, in which clean air (11-14 lpm) was constantly added to make up for instrument sample flow. ~~clean air was continuously added to the chamber to keep its volume constant~~. The temperature of the chamber was controlled at 292 (+/- 1) K. ~~and approximately 2% relative humidity~~. All experiments were carried out under dry conditions (relative humidity, RH ≅2%, +/- 1%) to simplify gas- and particle-phase measurements. Higher RH can potentially shorten the lifetime of particle-phase hydroperoxides, epoxides, and organonitrates (Li et al., 2018) as well as affect gas-particle partitioning kinetics and thermodynamics (Saukko et al., 2012).

We performed a series of photochemical experiments, in which toluene and 1,2,4-TMB were oxidized by OH ~~under high-NO conditions~~ (Table S1). The experiments were carried out under high-NO conditions such that the fate of peroxy radicals was primarily determined by their reaction with NO (Seinfeld and Pandis, 2016). First, dry ammonium sulfate particles, used as condensation nuclei, were injected in the chamber to reach a number concentration of 2.5-5.7·10^4 cm^{-3}. Seed particles were not injected into the chamber in two experiments. Hexafluorobenzene, (C_6F_6, which serves as a dilution tracer) was then added to the chamber. Next, nitrous acid (HONO) was ~~later~~ injected as an OH precursor. HONO was generated in a bubbler containing a solution of sodium nitrite by adding 2-4 μL of sulfuric acid via a syringe pump. 15 lpm of subsequently injected purified air carried HONO into the chamber, which resulted in a mixing ratio ~~concentration~~ of 28-35 ~~35-45~~ ppbv (except experiment 8 in which the initial HONO mixing ratio was 60 ppbv). ~~The concentration of NO in the chamber was estimated~~

~~to be ~0.3 ppbv while NO_2 concentration was approximately 10 ppbv.~~ After the addition of the oxidant, the aromatic precursor (toluene or 1,2,4-TMB, Sigma-Aldrich) was added to the chamber by injecting 3 μL of the precursor into a heated inlet. The initial mixing ratio ~~concentration~~ of the precursor was 89 ppbv in toluene experiments and 69 ppbv in 1,2,4-TMB experiments. The reagents were allowed to mix for several minutes, after which the ultraviolet (UV) lights, centred ~340 nm, were turned on to start photolysis of HONO (resulting in the production of hydroxyl radicals and nitric oxide) and photooxidation of the precursor. During experiments, additional injections of HONO were added to the chamber in order to roughly maintain the OH levels. As a result, the mixing ratio of NO in the chamber during experiments was estimated to be ~0.3 ppbv while the NO_2 mixing ratio was approximately 10 ppbv (Fig. S2). Measurements were conducted within several hours, corresponding to 14-16 hours of atmospheric-equivalent exposure (assuming an average OH concentration of $1.5 \cdot 10^6$ molecules cm^{-3}). Concentrations of O_3 and HONO+NO_x for a typical run are shown in Fig S2 ~~S1~~.

2.2 Chamber instrumentation

The concentration of ~~nitrogen oxides (NO_x) and HONO (42i NO_x monitor, Thermo Fisher Scientific),~~ ozone (2B Technologies), relative humidity, and temperature were measured in the chamber. A 42i NO_x monitor (Thermo Fischer Scientific) was used to measure the sum of concentrations of HONO and nitrogen oxides (NO_x). ~~Aromatic precursors as well as gas-phase oxygenated volatile organic compounds (OVOCs) were detected by chemical ionization high-resolution time-of-flight mass spectrometry (CIMS) instruments, including the I^- CIMS instrument (Aerodyne Research Inc.; Lee et al., 2014) and two proton transfer reaction mass spectrometry (PTR-MS) instruments: Vocus 2R PTR-TOF (TOFWERK A.G.; Krechmer et al., 2018) and PTR3 (Ionicon Analytik; Breitenlechner et al., 2017). The latter instrument was operated in a switching mode regime using $H_3O^+ \cdot (H_2O)_n$, n=0-1 (as H_3O^+ CIMS) and $NH_4^+ \cdot (H_2O)_n$, n = 0-2 (as NH_4^+ CIMS) primary ions (Hansel et al., 2018; Zaytsev et al., 2019). Switching between ion modes occurred every five minutes.~~ Aromatic precursors as well as gas-phase oxygenated volatile organic compounds (OVOCs) were detected by chemical ionization high-resolution time-of-flight mass spectrometry (CIMS) techniques: I^- CIMS, NH_4^+ CIMS, and H_3O^+ CIMS. The I^- CIMS instrument (Aerodyne Research Inc.) is described by Lee et al. (2014). NH_4^+ CIMS and H_3O^+ CIMS were carried out using a mass spectrometer (PTR3, Ionicon Analytik) which was operated in two ionization modes: $H_3O^+ \cdot (H_2O)_n$, n=0-1 (as PTR3 H_3O^+ CIMS, Breitenlechner et al., 2017) and $NH_4^+ \cdot (H_2O)_n$, n=0-2 (as PTR3 NH_4^+ CIMS, Zaytsev et al., 2019). Switching between ion modes occurred every five minutes. H_3O^+ CIMS was also conducted by a proton-transfer-reaction mass spectrometer (Vocus-2R-PTR, Aerodyne Research Inc.; Krechmer et al., 2018). Each CIMS instrument used a 3/16'' PFA Teflon sampling line of 1 m in length with a flow of 2 slm. PTR3 and Vocus-2R-PTR-TOF are designed to minimize inlet losses of sampled compounds (Krechmer et al., 2018; Breitenlechner et al., 2017); for more details see the Supplement. Detection efficiency and sensitivity of CIMS instruments depend critically on both the reagent ion and the measured sample molecule. The concentrations of aromatic precursors were measured by Vocus-2R-PTR-TOF, which was directly calibrated for the two compounds. Smaller, less oxidized molecules were primarily quantified by PTR-MS (PTR3 H_3O^+ CIMS and Vocus-2R-PTR-TOF) while PTR3 NH_4^+ CIMS and I^- CIMS were mainly used for detection of larger and more functionalized molecules. PTR3

and I^- CIMS instruments were directly calibrated for 10 VOCs with various functional groups (Tables S2 and S3). An average calibration factor was applied to other species detected by PTR-MS instruments, while collision-dissociation methods were implemented to constrain sensitivities of I^- CIMS and NH_4^+ CIMS (Lopez-Hilfiker et al., 2016; Zaytsev et al., 2019). Use of these methods and average calibration factors leads to uncertainties in estimated concentrations of detected compounds within a factor of ten. NH_4^+ CIMS uncertainties are within a factor of three while I^- CIMS is less certain. The majority of analysis in this work relies on NH_4^+ CIMS and PTR-MS data while I^- CIMS data are used as supporting measurements. ~~CO and formaldehyde were measured by tunable infrared laser differential absorption spectroscopy (TILDAS; Aerodyne Research Inc.), and~~ Glyoxal was detected by laser induced phosphorescence (Madison LIP; Huisman et al., 2008).

Total organic aerosol mass was measured using an Aerodyne Aerosol Mass Spectrometer (AMS, DeCarlo et al., 2006), calibrated with ammonium nitrate and assuming a collection efficiency of 1. Particle-phase compounds were quantified using the FIGAERO-HRToF-I^- CIMS (Lopez-Hilfiker et al., 2014), and a second PTR3 that could be operated in two positive modes as described above and equipped with an aerosol inlet comprising a gas-phase denuder and a thermal desorption unit heated to 180°C (TD-NH_4^+ CIMS and TD-H_3O^+ CIMS). At this temperature, all particles were evaporated while thermal decomposition of labile oxygenated compounds was relatively small (Zaytsev et al., 2019). Uncertainties of the particle-phase CIMS measurements are similar to the corresponding uncertainties of the gas-phase CIMS instruments.

2.3 Kinetic model

The Framework for 0-D Atmospheric Modelling v3.1 (F0AM; Wolfe et al., 2016) containing reactions from the Master Chemical Mechanism (MCM v3.3.1) (Jenkin et al., 2003; Bloss et al., 2005) was used to simulate photooxidation of 1,2,4-TMB and toluene in the environmental chamber and to compare the modelled products with the measurements. Model calculations were constrained to physical parameters of the environmental chamber (pressure, temperature, photolysis frequencies and dilution rate ~~calculated using the hexafluorobenzene tracer~~). The dilution term for volatile compounds was estimated based on the concentration of the dilution tracer, hexafluorobenzene. Injections of aromatic compounds and HONO were modelled as sources during the time of injection, and the chamber lights intensity was tuned to match the measured time-dependent concentration of aromatic precursors with the modelled values. ~~The chamber wall loss and dilution term for volatile compounds was estimated based on the concentration of the dilution tracer, hexafluorobenzene~~. As for semi- and low-volatile compounds, the wall deposition rate was estimated to be $5 \cdot 10^{-4}$ s^{-1} using the "rapid burst" method described in detail by Krechmer et al. (2016).

2.4 Calculation of OH exposure and product yields

The OH concentration was determined using the decay of the aromatic precursor, accounting for losses from dilution ~~and chamber wall deposition~~. The mixing ratio of the aromatic VOC (ArVOC: toluene or 1,2,4-TMB) is given by the following kinetics equation:

$$[\mathrm{ArVOC}]_t = [\mathrm{ArVOC}]_0 \cdot \exp\left(-k_{\mathrm{ArVOC+OH}} \cdot [\mathrm{OH}_{\mathrm{exposure}}]_t - k_{\mathrm{dilution\ ~~physical\ loss\ ArVOC~~}} \cdot t\right) \quad (1)$$

where [ArVOC] is the time-dependent mixing ratio of the aromatic precursor, $k_{\mathrm{ArVOC+OH}}$ is the second-order rate constant for ArVOC + OH reaction ($k_{\mathrm{toluene+OH}}$ = 5.63·10^{-12} cm^3 molecule^{-1} s^{-1} and $k_{1,2,4-\mathrm{TMB+OH}}$ = 3.25·10^{-11} cm^3 molecule^{-1} s^{-1} at 293K (Calvert et al., 2002)), $[\mathrm{OH}_{\mathrm{exposure}}]_t = \int_o^t [\mathrm{OH}]d\tau$ is the integrated OH exposure, k_{dilution} ~~physical loss ArVOC~~ is the unimolecular rate constant determining dilution ~~and chamber wall loss~~, and *t* is the time since the beginning of irradiation by the UV lights.

Yields of first-generation products were determined based on the decay of the aromatic precursor, rise of the product, and accounting for physical (dilution and chamber wall deposition) and chemical losses (reaction with OH, NO_3, O_3 and photolysis). A correction procedure described in detail by Galloway et al. (2011) is applied to calculate product yields. This correction takes into account physical and chemical losses of products in the environmental chamber:

$$[\mathrm{X}]_i^{\mathrm{corr}} = [\mathrm{X}]_{i-1}^{\mathrm{corr}} + \Delta[\mathrm{X}]_i + [\mathrm{X}]_{i-1}\Delta t(k_{\mathrm{chemical\ loss}} + k_{\mathrm{physical\ loss}}) \quad (2)$$

where $[\mathrm{X}]_i^{\mathrm{corr}}$ is the corrected mixing ratio of the compound at measurement time *i*, Δt is time between measurements *i* and *i* – 1, $[\mathrm{X}]_{i-1}$ is the measured product mixing ratio of measurement *i* – 1, $\Delta[\mathrm{X}]_i$ is the observed net change in [X] that occurs over Δt, $k_{\mathrm{chemical\ loss}}$ and $k_{\mathrm{physical\ loss}}$ are the rate constants describing chemical and physical losses of the product.

Yields of first-generation products were determined from the linear relationship between the amount of the corrected product formed and the amount of the primary ArVOC reacted:

$$[\mathrm{X}]^{\mathrm{corr}} = Y[\mathrm{ArVOC}]^{\mathrm{reacted}} ~~+ b~~ \quad (3)$$

where $[\mathrm{X}]^{\mathrm{corr}}$ is the amount of the corrected product formed, $[\mathrm{ArVOC}]^{\mathrm{reacted}}$ is the amount of the primary ArVOC reacted and *Y* is the first-generation yield of the product.

2.5 Gamma kinetics parameterization

Photooxidation products can be characterized not only by their concentration and yield, but also by their time series behaviour. In a laboratory experiment, the time series behaviour of a product is dependent on the kinetic parameters of the molecule: the relative rates of formation and reactive loss, and the number of reactions to create the product. We characterize time series behaviour of products using the gamma kinetics parametrization (GKP), which describes kinetics of an oxidation system in terms of multigenerational chemistry. The detailed description of this parametrization technique is given by Koss et al. (2019), so we include only a brief description here. A multigenerational hydroxyl radical oxidation system can be represented as a linear system of reactions:

$$\mathrm{X}_0 \xrightarrow{k\cdot[\mathrm{OH}]} \mathrm{X}_1 \xrightarrow{k\cdot[\mathrm{OH}]} \mathrm{X}_2 \xrightarrow{k\cdot[\mathrm{OH}]} \ldots \xrightarrow{k\cdot[\mathrm{OH}]} \mathrm{X}_m \xrightarrow{k\cdot[\mathrm{OH}]} \mathrm{X}_{m+1} \xrightarrow{k\cdot[\mathrm{OH}]} \ldots \quad (4)$$

where *k* is the second-order rate constant and *m* is the number of reactions needed to produce species X_m.

In laboratory experiments, oxidation reactions can be parametrized as a linear system of first-order reactions if reaction time *t* is replaced by OH exposure $[\mathrm{OH}_{\mathrm{exposure}}]_t = \int_0^t [\mathrm{OH}]d\tau$. In this case, the time-dependent concentration of a compound X_m can be parametrized by (Koss et al., 2019):

$$[X_m](t) = a(k \cdot [OH_{exposure}]_t)^m e^{-k \cdot [OH_{exposure}]_t} \quad (5)$$

where a is a scaling factor, k is the effective second-order rate constant (cm^3 molecule^{-1} s^{-1}), m is the generation number, and $[OH_{exposure}]_t$ is the integrated OH exposure (molecule s cm^{-3}).

Eq. (5) can be used to fit the observed concentration of a compound to return its parameters a, k and m. The parameter m determines the number of reactions with OH needed to produce the compound while the parameter k gives an approximate measure of the compound reactivity. We define "generation" here as the number of reactions with OH. At low generations (m = 1-2), the standard deviation of the fit is 0.1, while it can be higher (up to 0.8) at higher (3+) generations (Koss et al., 2019). Examples of fitted chamber measurements are shown in Fig. S3 ~~S2~~.

3 Results and discussion

Toluene and 1,2,4-TMB react with OH to form both ring-retaining (via benzaldehyde, phenolic and bicyclic channels) and ring scission (via bicyclic and epoxide channels) products. (~~The toluene oxidation scheme from MCM v3.3.1 is shown on Fig. 1.~~ These four channels are illustrated using the example of toluene in Fig. 1.) First and later-generation gas- and particle-phase oxidation products are detected and quantified for both systems. In the following sections we compare products suggested by MCM and previous studies to corresponding molecular formulas detected by CIMS. In some cases, the ion identity is well established from previous research or because there are a limited number of reasonable structures (e.g., phenols, benzaldehydes and ring-scission dicarbonyl products); in other cases, multiple isomers are possible, which could contribute to some differences between modelled and observed behaviour.

3.1 Products from benzaldehyde, phenolic and epoxide channels

In the toluene experiments, the approximate yields of benzaldehyde and cresol (~0.10 and ~0.16, respectively) were calculated based on the decay of toluene measured by Vocus-2R-PTR-TOF, rise of the two products measured by PTR3 H_3O^+ CIMS and NH_4^+ CIMS (cresol was measured by H_3O^+ CIMS while NH_4^+ CIMS was used for detecting benzaldehyde), and accounting for losses of cresol and benzaldehyde from wall deposition and reaction with OH and NO_3 (Sect 2.4). MCM v3.3.1 recommends a 0.07 yield of benzaldehyde and a 0.18 yield of cresol (total of all isomers) from OH initiated oxidation of toluene. Benzaldehyde and cresol concentrations predicted by MCM agree within uncertainties with the PTR3 H_3O^+ CIMS and NH_4^+ CIMS measurements, and the time-series behaviour of measurements and kinetic model predictions is similar (Fig. 3a). In general, MCM predicts that phenolic and benzaldehyde channels are less important for more substituted aromatics (Bloss et al., 2005). Hence, the MCM-based kinetic model recommends a 0.06 yield of dimethylbenzaldehyde and a 0.03 yield of trimethylphenol from the OH-initiated oxidation of 1,2,4-TMB. The kinetic model predictions for the two products agree within uncertainties with the ~~PTR-MS~~ H_3O^+ CIMS measurements and the time series behaviour is again similar (Fig. 3b). Phenols and benzaldehydes can further react within the MCM v3.3.1 scheme to form highly oxidized second-generation compounds. The importance of this pathway is discussed further in section 3.2.1.

MCM v3.3.1 also includes an epoxy-oxy channel in which it predicts formation of non-fragmented ~~non-fragmentary~~ linear epoxide-containing products (Fig. 1). The MCM-predicted yields of these species are 0.10 and 0.30 for toluene and 1,2,4-TMB systems, respectively. The ~~observed~~ yields of these products observed with NH_4^+ CIMS are significantly smaller (~0.01 in both systems). The observations are however consistent with theoretical studies (Li and Wang, 2014; Wu et al., 2014) in which it has been shown that only a negligible fraction of the bicyclic radicals would break the -O-O- bond to form epoxide-containing products.

3.2 Products from bicyclic pathway

3.2.1 Non-fragmented, ring-retaining products

Bicyclic peroxy radicals ~~(BPRs)~~ are formed through the addition of O_2 to the OH-adducts (Fig. 1). Starting from a generic aromatic compound C_xH_y, we expect the formation of BPRs with the formula $C_xH_{y+1}O_5$. BPRs likely react with RO_2, HO_2, or NO leading to the following products (Fig. 2) (Birdsall and Elrod, 2011): bicyclic carbonyls ($C_xH_yO_4$), bicyclic alcohols ($C_xH_{y+2}O_4$), bicyclic hydroperoxides ($C_xH_{y+2}O_5$), and bicyclic organonitrates ($C_xH_{y+1}NO_6$), as well as alkoxy radicals (discussed later). A number of oxygenated products is detected by NH_4^+ CIMS including $C_7H_8O_4$, $C_7H_{10}O_5$ and $C_7H_9NO_6$ in the toluene experiments, and $C_9H_{12}O_4$, $C_9H_{14}O_4$ and $C_9H_{13}NO_6$ in the 1,2,4-TMB experiments (Table 3). Since authentic standards are not available, ~~quantification of~~ these compounds were quantified ~~was done~~ using a voltage scanning procedure based on collision-induced dissociation (Sect. 2.2). The majority of OVOCs with high carbon numbers were detected at the maximum sensitivity, which was experimentally determined in each photooxidation experiment and depends on operational conditions of the NH_4^+ CIMS instrument (Zaytsev et al., 2019) (Tables S4 ~~S2~~ and S5 ~~S3~~). A number of products with the same molecular formulas corresponding to bicyclic carbonyls ($C_7H_8O_4$ and $C_9H_{12}O_4$) and alcohols ($C_7H_{10}O_4$ and $C_9H_{14}O_4$) were also detected by I^- CIMS and PTR-MS.

In MCM v3.3.1, the bicyclic peroxy radical undergoes analogous reactions: (1) it can react with HO_2 producing a hydroperoxide; (2) it can react with RO_2 producing an alkoxy radical, an alcohol or a carbonyl; (3) it can react with NO producing an alkoxy radical or a nitrate. According to MCM, under relevant urban conditions BPRs nearly exclusively react with NO and HO_2 and dominantly form alkoxy radicals which further decompose to smaller ring scission compounds (Figs. 2, S4 ~~S3~~ and S5 ~~S4~~) (Sect. 3.2.3). In this study, the approximate lifetime of BPRs, calculated as inverse reactivity, is estimated to be ~5 s for toluene and ~7 s for 1,2,4-TMB. MCM v3.3.1 does not include formation of the bicyclic carbonyl, $C_9H_{12}O_4$, in the 1,2,4-TMB oxidation scheme, while in the case of toluene it predicts that a major fraction of bicyclic carbonyl $C_7H_8O_4$ is produced as a second-generation product from the reaction of bicyclic hydroperoxide and organonitrate with OH. In contrast, the GKP fit based on the NH_4^+ CIMS measurements implies that a significant fraction of detected compounds is formed in the first generation in both systems (Table 3). These first-generation bicyclic carbonyls can be produced by the reaction of BPR with HO_2 or RO_2. In addition, MCM predicts higher than observed ~~significantly underestimates the~~ concentration of bicyclic alcohol ($C_9H_{14}O_4$ for 1,2,4-TMB system) since the only channel present in the MCM-based kinetic model is a reaction of BPR

with RO_2 while it can also be produced via the BPR+HO_2 pathway (Fig. 2). Finally, MCM v3.3.1 predicts that a notable fraction of BPR reacts with HO_2 to form bicyclic hydroperoxide. NH_4^+ CIMS measurements of $C_9H_{14}O_5$ and $C_7H_{10}O_5$ are less than the kinetic model prediction for each chemical system but agree within measurement uncertainties. The generation number *m* of $C_7H_{10}O_5$ and $C_9H_{14}O_5$ is ~1.7-1.8 which suggests that a compound with the same molecular formula can be produced by more than one pathway with different number of reaction steps. Birdsall and Elrod (2011) proposed that the BPR from several aromatic precursors reacting with HO_2 can form an alkoxy radical and OH. Similarly, recent studies have shown that numerous peroxy radicals do not form a hydroperoxide in unity yield while reacting with HO_2 (Praske et al., 2015; Orlando and Tyndall, 2012). Hence, we observe formation of numerous highly oxygenated compounds with molecular formula corresponding to bicyclic carbonyls, alcohols, organonitrates, and hydroperoxides via the peroxide-bicyclic channel under high-NO conditions. In addition to the formation of closed-shell products, bicyclic peroxy radicals can undergo isomerization reactions to form more oxidized peroxy radicals (Fig. 2) (Wang et al., 2017; Molteni et al., 2018). These reactions are not included in MCM v3.3.1. These radicals can in turn react with RO_2, HO_2, or NO leading to a series of more oxidized bicyclic products, so-called highly oxygenated molecules (HOMs): carbonyl ($C_xH_yO_6$), alcohol ($C_xH_{y+2}O_6$), hydroperoxide ($C_xH_{y+2}O_7$), and nitrate ($C_xH_{y+1}NO_8$). Several products with the aforementioned molecular formulas are detected by NH_4^+ CIMS (Fig. 4). In the toluene experiments, $C_7H_8O_6$, $C_7H_{10}O_6$, and $C_7H_9NO_8$ were detected by NH_4^+ CIMS as (NH_4^+)·OVOC. In the 1,2,4-TMB experiments, $C_9H_{14}O_6$, and $C_9H_{13}NO_8$ were detected as (NH_4^+)·OVOC while $C_9H_{12}O_6$ was detected both as $(NH_4^+)\cdot C_9H_{12}O_6$ (m/z 234.098) and as $[(NH_4)\cdot(H_2O)\cdot C_9H_{12}O_6]^+$ (m/z 252.108). The yield of molecules with a high O:C (greater than 0.44) ratio is larger in the case of 1,2,4-TMB compared to toluene. However, the gamma kinetics parametrization suggests that none of these compounds are solely first-generation products (Table 3) which implies that there are multiple chemical pathways in which products with the same molecular formula (but potentially different structure) are formed. Some of the products can be produced in the bicyclic oxidation pathway of cresol or trimethylphenol resulting in formation of alcohols ($C_xH_{y+2}O_5$), hydroperoxides ($C_xH_{y+2}O_6$) and nitrates ($C_xH_{y+1}NO_7$). Formation of bicyclic alcohols and hydroperoxides from the phenolic channel is included in MCM v3.3.1. We conclude that although a plethora of compounds with a high O:C ratio was observed, only some of them are formed via first-generation isomerization/autooxidation pathways. These findings underline the importance of phenolic and benzaldehyde channels for producing highly oxygenated compounds especially for the less substituted aromatics given the high yields of phenols and benzaldehydes and their high reactivity.

3.2.2 Fragmented ring-retaining products

In addition to non-fragmented functionalized C_9 and C_7 products possibly formed via the bicyclic channel, a variety of lower-carbon containing (C_8 and C_6) products with fewer carbon atoms were also detected in both chemical systems. The total concentration of C_8 components predicted by MCM v3.3.1 for 1,2,4-TMB is in good agreement with the NH_4^+ CIMS and ~~PTR-MS~~ H_3O^+ CIMS measurements (less oxidized compounds (O:C < 0.25) were detected using H_3O^+ CIMS while NH_4^+ CIMS was used for more oxidized species), though the observed composition is distinctly different from the MCM prediction (Fig. 5). According to MCM, there are only four C_8 products with mixing ratios at or above the ppt level. The most abundant

predicted compound, bicyclic carbonyl ($C_8H_{10}O_4$, MXYOBPEROH in MCM), is produced via the reaction of bicyclic nitrate $C_9H_{13}NO_6$ with OH, while the second most abundant compound, dimethylnitrophenol ($C_8H_9NO_3$, DM124OHNO2 in MCM), is formed in the benzaldehyde pathway. While all of the predicted products have been observed, NH_4^+ CIMS and PTR-MS also detect a plethora of C_8 compounds not included in MCM. Furthermore, MCM only predicts a total of 0.16 ppb for all C_6 compounds in the toluene experiments, while the combined measured mixing ratio of 15 C_6 compounds is ~0.5 ppb (Fig S6 ~~S5~~). The two most prominent C_6 products recommended by MCM, $C_6H_5NO_3$ and $C_6H_6O_2$, are predicted to be formed in the benzaldehyde channel.

There are several pathways that may lead to the formation of the fragmented ring-retaining C_8 and C_6 products. One of them is ipso addition followed by dealkylation (Loison et al., 2012). In their study of the dealkylation pathway in the OH-initiated oxidation of several aromatic compounds, Noda et al. (2009) showed the importance of this pathway and reported dealkylation yields of 0.054 for toluene. Similarly, Birdsall and Elrod determined a 0.047 yield of dealkylation products for toluene. Loison et al. (2012) reported a 0.02 yield of dealkylation pathway products from the hexamethylbenzene + OH reaction. However, in some studies yields of dealkylation products have been found below 0.01 (Aschmann et al., 2010). While we cannot determine exact yields of observed dealkylation compounds since many of them are later-generation products, we estimate an overall amount of carbon of ~3 ppbC and ~5 ppbC stored in C_6 and C_8 compounds for toluene and 1,2,4-TMB, respectively, compared to 600 ppbC in the system as a whole. Although observed concentrations of these products are not very high, a significant fraction (> 40%) of them are highly oxygenated products with an O:C ratio greater than 0.5. These products can effectively partition to the particle phase and contribute to SOA formation (Section 3.3).

3.2.3 Products from ring scission pathway

Recent theoretical studies suggest that the ring scission pathway leads to a series of two ring scission products such that the total number of carbon atoms present in the original aromatic compound is conserved in the two products (Wu et al., 2014; Li and Wang, 2014). In particular, a toluene study by Wu et al. (2014) predicts significant yields of 1,2-dicarbonyls and a range of C_4 and C_5 products. Those larger compounds include dicarbonyls (butenedial $C_4H_4O_2$ and methylbutenedial $C_5H_6O_2$), which were already detected in previous experimental studies (Calvert et al., 2002), and newly proposed epoxy-dicarbonyl products (epoxybutanedial $C_4H_4O_3$ and methylepoxybutanedial $C_5H_6O_3$). As for 1,2,4-TMB, Li and Wang (2014) also predict two groups of ring scission products: (1) smaller 1,2-dicarbonyls such as glyoxal, methylglyoxal and biacetyl and (2) larger C_5, C_6 and C_7 products. Similar to the toluene system, those larger compounds include dicarbonyls ($C_5H_6O_2$, $C_6H_8O_2$ and $C_7H_{10}O_2$), which were previously reported in numerous studies, and new epoxy-dicarbonyl products ($C_5H_6O_3$ and $C_6H_8O_3$). Some experimental studies reported that larger ring scission products were found at systematically lower yields than the corresponding 1,2-dicarbonyl products (Arey et al., 2009). This result suggests that either the product pair carbon conservation rule is not followed or that the larger products undergo further photochemical or heterogeneous degradation in the environmental chamber.

A series of ~~1,2-~~dicarbonyls were experimentally detected including glyoxal and methylglyoxal in the toluene experiments, and methylglyoxal and biacetyl in the 1,2,4-TMB experiments (Tables 1 and 2). Although a relatively small amount of glyoxal (2.5 ppb) is predicted to be formed from the 1,2,4-TMB + OH pathway, observed amounts of glyoxal were below the limit of detection of the Madison LIP instrument (1 ppb) suggesting that the glyoxal yield does not exceed 0.03 in this system. Measured glyoxal and methylglyoxal formation yields, combined with the biacetyl yield from the 1,2,4-TMB oxidation, indicate that under high-NO conditions the first-generation yield of all 1,2-dicarbonyls is ~0.43 and ~0.35 for toluene and 1,2,4-TMB, respectively (Tables 1 and 2). For all 1,2-dicarbonyls the observed generation number *m* is greater than 1 and is consistent between the two systems, which suggests that these compounds are produced by more than one pathway with different numbers of reaction steps. In addition to the aforementioned 1,2-dicarbonyls, a series of dicarbonyls with a higher carbon number was observed in both systems (Tables 1 and 2). For all these species (except trimethylbutenedial) the generation number *m* is slightly smaller than 1. Finally, ions corresponding to newly proposed epoxy-dicarbonyl products were also observed (Tables 1 and 2). However, the generation number *m* for these compounds is between 1 and 2, suggesting that there are multiple pathways resulting in compounds with those molecular formulas. Overall, we observed ~0.45 and ~0.47 yields of larger carbonyls in the toluene and 1,2,4-TMB experiments, respectively.

3.3 SOA Analysis

Peak SOA concentration measured by TD-NH_4^+ CIMS was 1.8 μg m^{-3} for the toluene oxidation experiment and 1.4 μg m^{-3} for 1,2,4-TMB which is in good agreement with the AMS measurements (1.9 μg m^{-3} and 1.6 μg m^{-3}, respectively). Figure 6 depicts the relative distribution of carbon in the particle phase according to the carbon atom number n_C for 1,2,4-TMB and toluene SOA, respectively. The O:C ratios calculated from individual species measured from thermally desorbed SOA using NH_4^+ CIMS were ~0.95 for toluene SOA and ~0.7 for 1,2,4-TMB SOA. These ratios are in good agreement with the atomic O:C ratios measured by AMS (0.85 and 0.65 for toluene and 1,2,4-TMB SOA, respectively) (Canagaratna et al., 2015).

Products observed in the gas phase are compared to those detected in the particle phase to further understand the mechanism of SOA formation from aromatics precursors. A variety of ring-retaining products were observed in the particle phase for oxidation of 1,2,4-TMB and toluene: non-fragmented ~~non-fragmentary~~ products (e.g., $C_9H_{12}O_{4\text{-}6}$ for 1,2,4-TMB and $C_7H_8O_{4\text{-}6}$ for toluene) and fragmentary products (e.g., $C_8H_{10}O_{4\text{-}5}$, $C_7H_8O_{4\text{-}5}$ for 1,2,4-TMB and $C_6H_6O_{4\text{-}5}$ for toluene). The same non-fragmentary ring-retaining oxidation products, detected by NH_4^+ CIMS in the gas phase and expected to be low in volatility, are detected in the particle phase (Fig. 4). Overall, ring-retaining products make up a significant fraction of the total 1,2,4-TMB SOA mass (~25% for 1,2,4-TMB SOA and ~30% for toluene SOA) (Fig. 6), even though the total concentration of these products in the gas phase is relatively small (~2 ppb for 1,2,4-TMB and ~1 ppb for toluene). Furthermore, numerous species ~~masses~~ corresponding to those of the ring scission products were detected including $C_5H_8O_3$, $C_4H_6O_3$, and $C_3H_4O_2$. It is likely that the concentration of larger ring-retaining products in the particle phase is underestimated due to their thermal fragmentation in the desorption unit inlet of the NH_4^+ CIMS instrument (Zaytsev et al., 2019) although it should be noted that many highly oxygenated compounds were detected, e.g., $C_7H_6O_6$ and $C_9H_{10}O_7$. These findings underscore the importance of

bicyclic, phenolic and benzaldehyde channels for producing ring-retaining highly oxygenated compounds that comprise a significant fraction of SOA (more than 25%).

4 Conclusions and implications for the aromatic oxidation mechanism

In the present work, we studied the multigenerational photooxidation of two aromatic compounds (toluene and 1,2,4-trimethylbenzene) in an environmental chamber under relevant urban high-NO conditions. We identified a number of oxidation products based on their molecular formula and determined yields for certain first-generation products. We provided kinetic and mechanistic information on numerous products using a gamma kinetics parameterization fit.

We compare and contrast observed products with predictions from the Master Chemical Mechanism (MCM v3.3.1), which provides explicit representation of chemical reactions that constitute the overall aromatic oxidation mechanism on the basis of the extensive body of existing experimental work. Laboratory studies are a vital support for the mechanism ~~model~~, and the agreement between these studies and the MCM output is one of the important criteria demonstrating the accuracy of the kinetic model prediction. MCM accurately predicts the overall presence and importance of the three major channels for the primary OH-initiated oxidation of aromatic compounds (peroxide-bicyclic, benzaldehyde and phenolic). However, the epoxy-oxy channel appears to be overpredicted by the MCM-based kinetic model. In both systems we observed a variety of stable bicyclic products which underlines the importance of the bicyclic channel in the oxidation of aromatic compounds (Fig. 1). MCM correctly predicts the greater importance of the bicyclic pathway for the more substituted aromatics, though the speciated fate of BPRs is not entirely consistent with observations. In addition to bicyclic organonitrates, carbonyls, and alcohols, we detect numerous compounds with molecular formulas corresponding to bicyclic hydroperoxides, which suggests that this class of products may be formed in the oxidation of aromatic molecules even under high-NO conditions. Recent studies (Molteni et al., 2018; Wang et al., 2017) suggest that bicyclic peroxy radicals can undergo isomerization and autooxidation reactions leading to the formation of HOMs. Furthermore, Molteni et al. (2018) report that the HOM yields from various aromatics are relatively uniform and are not linked to bicyclic peroxy radical or phenol formation yields. Here, we observe the formation of highly oxygenated compounds with a high O:C ratio (up to 1.1) in both systems. However, the abundance of these compounds is greater in the case of 1,2,4-TMB for which the yield of bicyclic peroxy radicals is higher (Fig. 4). Moreover, the observed kinetics of these compounds suggests that they might be produced by more than one pathway, including both the isomerization/autooxidation reactions and further oxidation of phenols and benzaldehydes. Many of these compounds are low in volatility and comprise a significant fraction (more than 25%) of SOA mass, which was measured using AMS and TD-NH_4^+ CIMS and the two measurements are in good agreement. These findings emphasize the significance of ring-retaining highly oxygenated products for SOA formation and provide further evidence that isomerization and autooxidation reactions can be fast enough to compete with bimolecular reactions with NO and HO_2 even under high-NO conditions (in this study the total BPR loss rate ~~reactivity~~ is estimated to be ~0.1-0.2 s^{-1} (Figs. S4 ~~S3~~ and S5 ~~S4~~)). A plethora of fragmentary ring-retaining products is observed in the gas phase in both systems, many of which are not present in MCM, which underlines the importance

of the fragmentation pathway in oxidation of aromatic compounds. Numerous ring scission products are detected, including C_2-C_7 dicarbonyls and $C_{4\text{-}6}H_{4\text{-}8}O_3$ products, possibly epoxydicarbonyls. The kinetics of the ring scission products (e.g., generation number *m*) is consistent between the two systems, which suggests that many of those carbonyls are produced in more than one pathway with differing number of reaction steps with OH, and those pathways are similar between different aromatic systems.

Competing interests. Authors declare no competing interests.

Author contributions. AZ, ARK, MB, JEK, KJN, CYL, JCR, JLC, JRR, and MRC collected and analysed data. ARK developed the GKP analysis. FNK and JHK provided project guidance. AZ prepared the manuscript with contributions from all co-authors.

Acknowledgments. This work was supported by the Harvard Global Institute, the NSF award AGS-1638672, and a core center grant P30-ES002109 from the National Institute of Environmental Health Sciences, National Institutes of Health. ARK acknowledges support from the Dreyfus Postdoctoral Program. MB acknowledges support from the Austrian science fund (FWF), grant J-3900.

References

Arey, J., Obermeyer, G., Aschmann, S.M., Chattopadhyay, S., Cusick, R.D., and Atkinson, R.: Dicarbonyl Products of the OH Radical-Initiated Reaction of a Series of Aromatic Hydrocarbons, Environ. Sci. Technol., 43, 3, 683-689, doi: 10.1021/es8019098, 2009.

Bianchi, F., Kurtén, T., Riva, M., Mohr, C., Rissanen, M.P., Roldin, P., Berndt, T., Crounse, J.D., Wennberg, P.O., Mentel, T.F., Wildt, J., Junninen, H., Jokinen, T., Kulmala, M., Worsnop, D.R., Thornton, J.A., Donahue, N., Kjaergaard, H.G., and Ehn M.: Highly Oxygenated Organic Molecules (HOM) from Gas-Phase Autoxidation Involving Peroxy Radicals: A Key Contributor to Atmospheric Aerosol, Chem. Rev. 119 (6), 3472–3509, doi:10.1021/acs.chemrev.8b00395, 2019.

Birdsall, A.W., Andreoni, J.F., and Elrod, M.J.: Investigation of the Role of Bicyclic Peroxy Radicals in the Oxidation Mechanism of Toluene, J. Phys. Chem. A, 114, 10655-10663, doi:10.1021/jp105467e, 2010.

Birdsall, A.W., and Elrod, M.J.: Comprehensive NO-Dependent Study of the Products of the Oxidation of Atmospherically relevant Aromatic Compounds, J. Phys. Chem. A, 115, 5397-5407, doi:10.1021/jp.2010327, 2011.

Bloss, C., Wagner, V., Jenkin, M. E., Volkamer, R., Bloss, W. J., Lee, J. D., Heard, D. E., Wirtz, K., Martin-Reviejo, M., Rea, G., Wenger, J. C., and Pilling, M. J.: Development of a detailed chemical mechanism (MCMv3.1) for the atmospheric oxidation of aromatic hydrocarbons, Atmos. Chem. Phys., 5, 641-664, doi:10.5194/acp-5-641-2005, 2005

Bohn B., and Zetzsch, C: Kinetics and mechanism of the reaction of OH with the trimethylbenzenes – experimental evidence for the formation of adduct isomers, Phys. Chem. Chem. Phys., 14, 13933–13948, doi: 10.1039/c2cp42434g, 2012.

Calvert, J., Atkinson, R., Becker, K.H., Kamens, R., Seinfeld, J., Wallington, T., and Yarwood, G.: The mechanisms of atmospheric oxidation of aromatic hydrocarbons, Oxford University Press, Inc., New York, 2002.

Canagaratna, M. R., Jimenez, J. L., Kroll, J. H., Chen, Q., Kessler, S. H., Massoli, P., Hildebrandt Ruiz, L., Fortner, E., Williams, L. R., Wilson, K. R., Surratt, J. D., Donahue, N. M., Jayne, J. T., and Worsnop, D. R.: Elemental ratio measurements of organic compounds using aerosol mass spectrometry: characterization, improved calibration, and implications, Atmos. Chem. Phys., 15, 253-272, doi:10.5194/acp-15-253-2015, 2015.

DeCarlo, P.F., Kimmel, J.R., Trimborn, A., Northway, M.J., Jayne, J.T., Aiken, A.C., Gonin, M., Fuhrer, K., Horvath, T., Docherty, K.S., Worsnop, D.R., and Jimenez, J.L.: Field-Deployable, High-Resolution, Time-of-Flight Aerosol Mass Spectrometer, Anal. Chem., 78 (24), 8281-8289, doi:10.1021/ac061249n, 2006.

Galloway, M. M., Huisman, A. J., Yee, L. D., Chan, A.W. H., Loza, C. L., Seinfeld, J. H., and Keutsch, F. N.: Yields of oxidized volatile organic compounds during the OH radical initiated oxidation of isoprene, methyl vinyl ketone, and methacrolein under high-NO_X conditions, Atmos. Chem. Phys., 11, 10779–10790, doi:10.5194/acp-11-10779-2011, 2011.

Hansel, A., Scholz, W., Mentler, B., Fischer L., and Berndt, T.: Detection of RO_2 radicals and other products from cyclohexene ozonolysis with NH_4^+ and acetate ionization mass spectrometry, Atmos. Env., 186, 248–255, 5 doi:10.1016/j.atmosenv.2018.04.023, 2018.

Huisman, A.J., Hottle, J.R., Coens, K.L., DiGangi, J.P., Galloway, M.M., Kammrath, A., and Keutsch., F.N.: Laser-Induced Phosphorescence for the in Situ Detection of Glyoxal at Part per Trillion Mixing Ratios, Anal. Chem., 80, 5884–5891, doi:10.1021/ac800407b, 2008.

Hu, D., Q. J. Bian, T. W. Y. Li, A. K. H. Lau, and J. Z. Yu (2008), Contributions of isoprene, monoterpenes, beta-caryophyllene, and toluene to secondary organic aerosols in Hong Kong during the summer of 2006, J. Geophys. Res.-Atmos., 113, D22206, doi:10.1029/2008JD010437, 2008.

Hunter, J.F., Carrasquillo, A.J., Daumit, K.E., and Kroll J.H.: Secondary Organic Aerosol Formation from Acyclic, Monocyclic, and Polycyclic Alkanes. Environ. Sci. Technol., 48, 10227−10234, doi:10.1021/es502674s, 2014.

Jang, M., and Kamens, R.M.: Characterization of Secondary Aerosol from the Photooxidation of Toluene in the Presence of NOx and 1-Propene, Environ. Sci. Technol., 35, 3626-3639, https://doi.org/10.1021/es010676+, 2001.

Jenkin, M. E., Saunders, S. M., Wagner, V., and Pilling, M. J.: Protocol for the development of the Master Chemical Mechanism, MCM v3 (Part B): tropospheric degradation of aromatic volatile organic compounds, Atmos. Chem. Phys., 3, 181–193, doi:10.5194/acp-3-181-2003, 2003.

Kleindienst, T.E., Conver, T.S., McIver, C.D., and Edney, E.O.: Determination of Secondary Organic Aerosol Products from the Photooxidation of Toluene and their Implications in Ambient PM2.5, Journal of Atmospheric Chemistry, 47, 79-100, https://doi.org/10.1023/B:JOCH.0000012305.94498.28, 2004.

Klotz, B., Sorensen, S., Barnes, I., Becker, K.-H., Etzkorn, T., Volkamer, R., Platt, U., Wirtz, K., and Martin-Reviejo, M.: Atmospheric Oxidation of Toluene in a Large-Volume Outdoor Photoreactor: In Situ Determination of Ring-Retaining Product Yields, J. Phys. Chem. A, 102, 10289−10299 doi:10.1021/jp982719n, 1998.

Koss, A.R., Canagaratna, M., Zaytsev, A., Krechmer, J.E., Breitenlechner, M., Nihill, K.J., Lim, C.Y., Rowe, J.C., Roscioli, J.R., Keutsch, F.N., and Kroll, J.H.: Dimensionality-reduction techniques for complex mass spectrometric datasets: application to laboratory atmospheric organic oxidation experiments, Atmos. Chem. Phys. Discuss., doi:10.5194/acp-2019-469, in review, 2019.

Krechmer, J.E., Pagonis, D., Ziemann, P.J., and Jimenez, J.L.: Quantification of Gas-Wall Partitioning in Teflon Environmental Chambers Using Rapid Bursts of Low-Volatility Oxidized Species Generated in Situ, Environ. Sci. Technol. 50(11), 5757−5765, doi:10.1021/acs.est.6b00606, 2016.

Krechmer, J.E., Lopez-Hilfiker, F., Koss, A., Hutterli, M., Stoermer, C., Deming, B., Kimmel, J., Warneke, C., Holzinger, R., Jayne, J., Worsnop, D., Fuhrer, K., Gonin, M., and de Gouw J.: Evaluation of a New Vocus Reagent-Ion Source and Focusing Ion-Molecule Reactor for use in Proton-Transfer-Reaction Mass Spectrometry, Anal. Chem., 90, 20, 12011-12018, doi:10.1021/acs.analchem.8b02641, 2018.

Lopez-Hilfiker, F. D., Mohr, C., Ehn, M., Rubach, F., Kleist, E., Wildt, J., Mentel, Th. F., Lutz, A., Hallquist, M., Worsnop, D., and Thornton, J. A.: A novel method for online analysis of gas and particle composition: description and evaluation of a Filter Inlet for Gases and AEROsols (FIGAERO), Atmos. Meas. Tech., 7, 983-1001, doi:10.5194/amt-7-983-2014, 2014.

Lopez-Hilfiker, F. D., Iyer, S., Mohr, C., Lee, B. H., D'Ambro, E. L., Kurtén, T., and Thornton, J. A.: Constraining the sensitivity of iodide adduct chemical ionization mass spectrometry to multifunctional organic molecules using the collision limit and thermodynamic stability of iodide ion adducts, Atmos. Meas. Tech., 9, 1505-1512, doi:10.5194/amt-9-1505-2016, 2016.

Li, Y., and Wang, L.: The atmospheric oxidation mechanism of 1,2,4-trimethylbenzene initiated by OH radicals, Phys. Chem. Chem. Phys., 16, 17908-17917, doi:10.1039/c4cp02027h, 2014.

Li, L., Tang, P., Nakao, S., and Cocker III, D. R.: Impact of molecular structure on secondary organic aerosol formation from aromatic hydrocarbon photooxidation under low-NO_x conditions, Atmos. Chem. Phys., 16, 10793-10808, doi:10.5194/acp-16-10793-2016, 2016.

Loison, J.-C., Rayez, M.-T., Rayez, J.-C., Gratien, A., Morajkar, P., Fittschen, C., and Villenave, E.: Gas-Phase Reaction of Hydroxyl Radical with Hexamethylbenzene, J. Phys. Chem. A, 116, 12189−12197, doi:10.1021/jp307568c, 2012.

Molteni, U., Bianchi, F., Klein, F., El Haddad, I., Frege, C., Rossi, M. J., Dommen, J., and Baltensperger, U.: Formation of highly oxygenated organic molecules from aromatic compounds, Atmos. Chem. Phys., 18, 1909-1921, doi:10.5194/acp-18-1909-2018, 2018.

Nishino, N., Arey, J., and Atkinson, R.: Formation Yields of Glyoxal and Methylglyoxal from the Gas-Phase OH Radical-Initiated Reactions of Toluene, Xylenes, and Trimethylbenzenes as a Function of NO2 Concentration, J. Phys. Chem. A, 114, 10140, doi:10.1021/jp105112h, 2010.

Noda, J., Volkamer R., and Molina M.J.: Dealkylation of Alkylbenzenes: A Significant Pathway in the Toluene, *o*-, *m*-, *p*-Xylene + OH Reaction, J. Phys. Chem. A, 113, 9658–9666, doi:10.1021/jp901529k, 2009.

Olariu, R. I., Klotz, B., Barnes, I., Becker, K. H., and Mocanu, R.: FT-IR study of the ring-retaining products from the reaction of OH radicals with phenol, o-, m-, and p-cresol, Atmos. Environ., 36, 3685–3697, 2002.

Orlando, J. J. and Tyndall, G. S.: Laboratory studies of organic peroxy radical chemistry: an overview with emphasis on recent issues of atmospheric significance, Chem. Soc. Rev., 41, 6294–6317, doi:10.1039/c2cs35166h, 2012.

Praske, E., Crounse, J.D., Bates, K.H., Kurtén, T., Kjaergaard, H.G., and Wennberg, P.O.: Atmospheric Fate of Methyl Vinyl Ketone: Peroxy Radical Reactions with NO and HO_2, J. Phys. Chem. A, 119 (19), 4562–4572, doi: 10.1021/jp5107058, 2015.

Saukko, E., Lambe, A. T., Massoli, P., Koop, T., Wright, J. P., Croasdale, D. R., Pedernera, D. A., Onasch, T. B., Laaksonen, A., Davidovits, P., Worsnop, D. R., and Virtanen, A.: Humidity-dependent phase state of SOA particles from biogenic and anthropogenic precursors, Atmos. Chem. Phys., 12, 7517-7529, https://doi.org/10.5194/acp-12-7517-2012, 2012.

Schwantes, R. H., Schilling, K. A., McVay, R. C., Lignell, H., Coggon, M. M., Zhang, X., Wennberg, P. O., and Seinfeld, J. H.: Formation of highly oxygenated low-volatility products from cresol oxidation, Atmos. Chem. Phys., 17, 3453-3474, https://doi.org/10.5194/acp-17-3453-2017, 2017.

Seinfeld, J.H., and Pandis, S.N.: Atmospheric Chemistry and Physics: From Air Pollution to Climate Change, Wiley, Hoboken NJ, 2016.

Smith, D. F., McIver, C. D., and Kleindienst, T. E.: Primary Product Distribution from the Reaction of Hydroxyl Radicals with Toluene at ppb NOx Mixing Ratios, J. Atmos. Chem., 30, 209−228, doi:10.1023/A:1005980301720, 1998.

Smith, D.F., Kleindienst, T.E., and McIver, D.F.: Primary Product Distributions from the Reaction of OH with *m*-, *p*-Xylene, 1,2,4- and 1,3,5-Trimethylbenzene, Journal of Atmospheric Chemistry, 34, 339, doi: 10.1023/A:1006277328628, 1999.

Tang, J.H., Chan, L.Y., Chan, C.Y., Li, Y.S., Chang, C.C., Wang, X.M., Zou, S.C., Barletta, B., Blake, D.R., and Wu, D.: Implications of changing urban and rural emissions on non-methane hydrocarbons in the Pearl River Delta region of China, Atmospheric Environment, 42, 3780–3794, doi:10.1016/j.atmosenv.2007.12.069, 2007.

Wang, S., Wu, R., Berndt, T., Ehn, M., and Wang, L.: Formation of Highly Oxidized Radicals and Multifunctional Products from the Atmospheric Oxidation of Alkylbenzenes, Environ. Sci. Technol., 51 (15), 8442–8449, doi:10.1021/acs.est.7b02374, 2017.

Wolfe, G.M., Marvin, M.M., Roberts, S.J., Travis, K.R., and Liao, J.: The Framework for 0-D Atmospheric Modeling (F0AM) v3.1, Geosci. Model Dev., 9, 3309-3319, doi:10.5194/gmd-2016-175, 2016.

Wu, R., Pan, S., Li, Y., and Wang, L.: Atmospheric Oxidation Mechanism of Toluene, J. Phys. Chem. A., 118, 4533-4547, https://doi.org/10.1021/jp500077f, 2014.

Wyche, K. P., Monks, P. S., Ellis, A. M., Cordell, R. L., Parker, A. E., Whyte, C., Metzger, A., Dommen, J., Duplissy, J., Prevot, A. S. H., Baltensperger, U., Rickard, A. R., and Wulfert, F.: Gas phase precursors to anthropogenic secondary organic aerosol: detailed observations of 1,3,5-trimethylbenzene photooxidation, Atmos. Chem. Phys., 9, 635-665, doi:10.5194/acp-9-635-2009, 2009.

Zaytsev, A., Breitenlechner, M., Koss, A. R., Lim, C. Y., Rowe, J. C., Kroll, J. H., and Keutsch, F. N.: Using collision-induced dissociation to constrain sensitivity of ammonia chemical ionization mass spectrometry (NH_4^+ CIMS) to oxygenated volatile organic compounds, Atmos. Meas. Tech., 12, 1861-1870, doi:10.5194/amt-12-1861-2019, 2019.

Zheng, J., Shao, M., Che, W., Zhang, L., Zhong, L., Zhang, Y., and Streets, D.: Speciated VOC emission inventory and spatial patterns of ozone formation potential in the Pearl River Delta, China, Environ. Sci. Technol., 43 (22), 8580–8586, doi:10.1021/es901688e, 2009.

Table 1: Major toluene oxidation products measured by PTR-MS and NH_4^+ CIMS.

Product Name	Product Formula	Generation parameter *m*	Kinetic parameter *k* (cm^3 $molecule^{-1}$ s^{-1})	Yield (%)
glyoxal	$C_2H_2O_2$	1.2	$1.3 \cdot 10^{-11}$	28%
methylglyoxal	$C_3H_4O_2$	1.3	$1.1 \cdot 10^{-11}$	15%
butenedial	$C_4H_4O_2$	0.8	$2 \cdot 10^{-11}$	8%
methylbutenedial	$C_5H_6O_2$	0.7	$2 \cdot 10^{-11}$	37%
epoxybutanedial	$C_4H_4O_3$	1.3	$1 \cdot 10^{-11}$	5%
methylepoxybutanedial	$C_5H_6O_3$	1.3	$1 \cdot 10^{-11}$	5%
benzaldehyde	C_7H_6O	1	$1 \cdot 10^{-11}$	9%
cresol	C_7H_8O	1	$2.3 \cdot 10^{-11}$	10%
dicarbonylepoxide	$C_7H_8O_3$	0.9	$2.2 \cdot 10^{-11}$	1%

Table 2: Major 124-TMB oxidation products measured by PTR-MS and NH_4^+ CIMS

Product Name	Product Formula	Generation parameter *m*	Kinetic parameter *k* (cm^3 $molecule^{-1}$ s^{-1})	Yield (%)
methylglyoxal	$C_3H_4O_2$	1.3	$1.8 \cdot 10^{-11}$	25%
biacetyl	$C_4H_6O_2$	1.3	$2.2 \cdot 10^{-11}$	10%
methylbutenedial	$C_5H_6O_2$	0.7	$3.5 \cdot 10^{-11}$	5%
dimethylbutenedial	$C_6H_8O_2$	0.9	$4.1 \cdot 10^{-11}$	40%
trimethylbutenedial	$C_7H_{10}O_2$	1	$5.1 \cdot 10^{-11}$	2%
methylepoxybutanedial	$C_5H_6O_3$	1.8	$1.9 \cdot 10^{-11}$	N/A
dimethylepoxybutanedial	$C_6H_8O_3$	1.1	$2.4 \cdot 10^{-11}$	2%
dimethylbenzaldehyde	$C_9H_{10}O$	1	$1.4 \cdot 10^{-11}$	3%
trimethylphenol	$C_9H_{12}O$	1	$3.5 \cdot 10^{-11}$	2%
dicarbonylepoxide	$C_9H_{12}O_3$	1	$4 \cdot 10^{-11}$	1%

Table 3: Kinetics fit of gas-phase highly oxygenated compounds detected in toluene (top five rows) and 1,2,4-TMB (bottom seven rows) oxidation experiments.

Product Formula	Generation parameter *m*	Kinetic parameter *k* (cm^3 $molecule^{-1}$ s^{-1})
$C_7H_8O_4$	1.5	$1 \cdot 10^{-11}$
$C_7H_{10}O_5$	1.5	$1 \cdot 10^{-11}$
$C_7H_8O_6$	1.6	$1.1 \cdot 10^{-11}$
$C_7H_9NO_6$	2.1	$0.8 \cdot 10^{-11}$
$C_7H_9NO_8$	2	$0.9 \cdot 10^{-11}$
$C_9H_{12}O_4$	1.5	$1.8 \cdot 10^{-11}$
$C_9H_{14}O_4$	1.6	$1.7 \cdot 10^{-11}$
$C_9H_{14}O_5$	1.8	$1.9 \cdot 10^{-11}$
$C_9H_{12}O_6$	1.8	$1.4 \cdot 10^{-11}$
$C_9H_{13}NO_6$	1.4	$1.7 \cdot 10^{-11}$
$C_9H_{13}NO_7$	2.1	$2.3 \cdot 10^{-11}$
$C_9H_{13}NO_8$	2.3	$1.8 \cdot 10^{-11}$

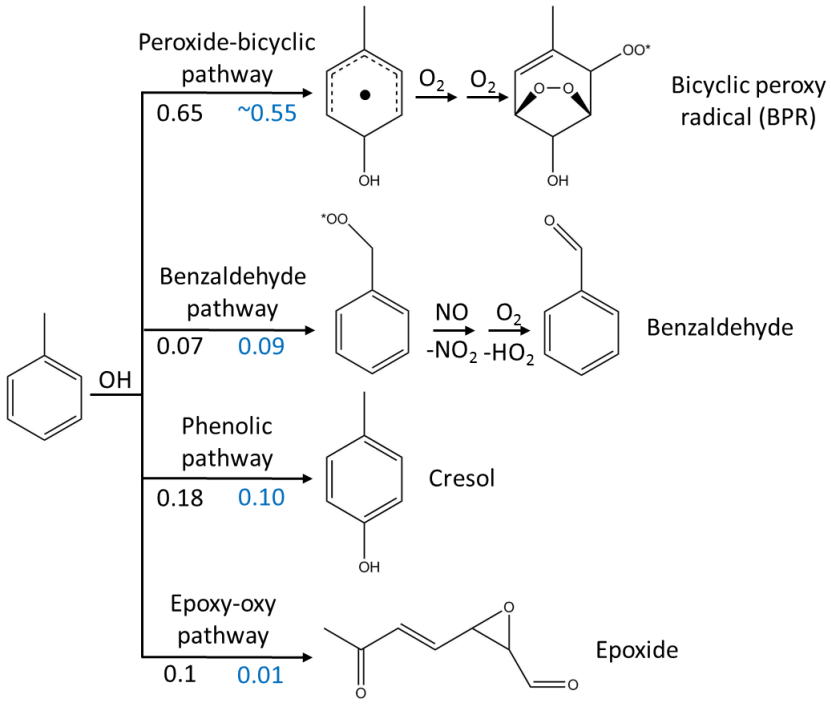

Figure 1: ~~Gas-phase chemical mechanism for toluene photooxidation.~~ **Major gas-phase oxidation pathways for aromatic hydrocarbons, using toluene as an example. Reaction yields for the** ~~major~~ **oxidation pathways of toluene recommended by MCM v3.3.1 are shown in black (Bloss et al., 2005). The proposed yields from the present study are shown in blue. The yield of the peroxide-bicyclic pathway is calculated based on the yields of ring-scission products.**

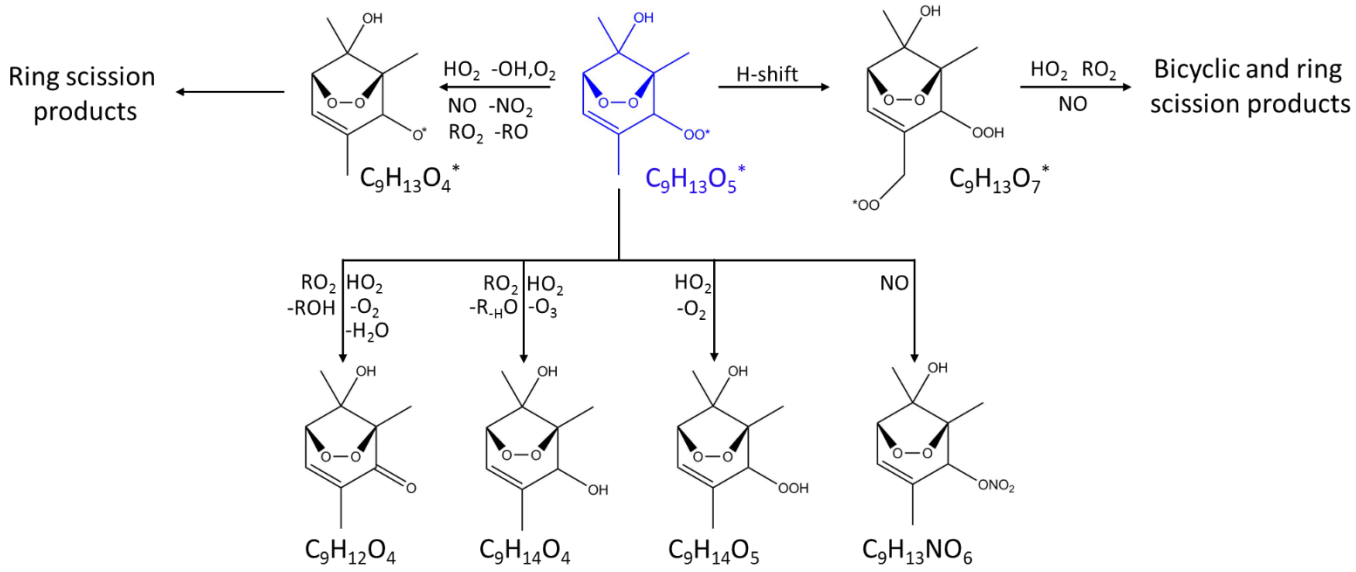

Figure 2: Oxidation pathways of bicyclic peroxy radicals in the OH-initiated oxidation of 1,2,4-trimethylbenzene. The starting radical us shown in blue. Bimolecular reactions are from MCM v3.3.1 (Bloss et al., 2005) and Birdsall and Elrod (2011).

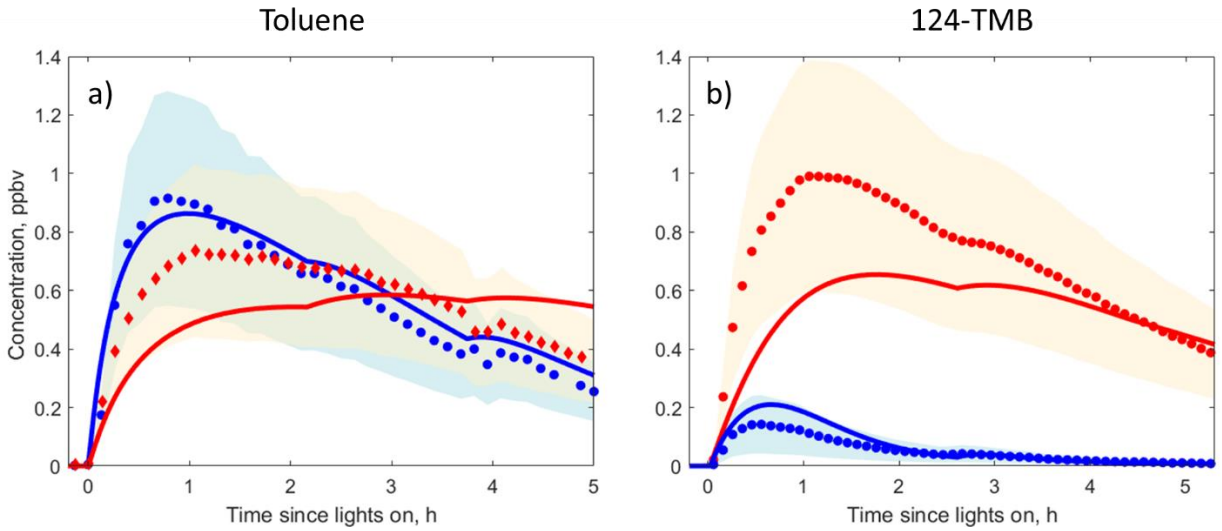

Figure 3: MCM v3.3.1 predictions (solid lines) compared to PTR-MS (circles) and NH_4^+ CIMS (diamonds) measurements under high-NO_x oxidation of (a) toluene and (b) 124-TMB for phenols (red) and benzaldehydes (blue). The uncertainty in the PTR-MS and NH_4^+ CIMS measurements is shown in blue and red shading.

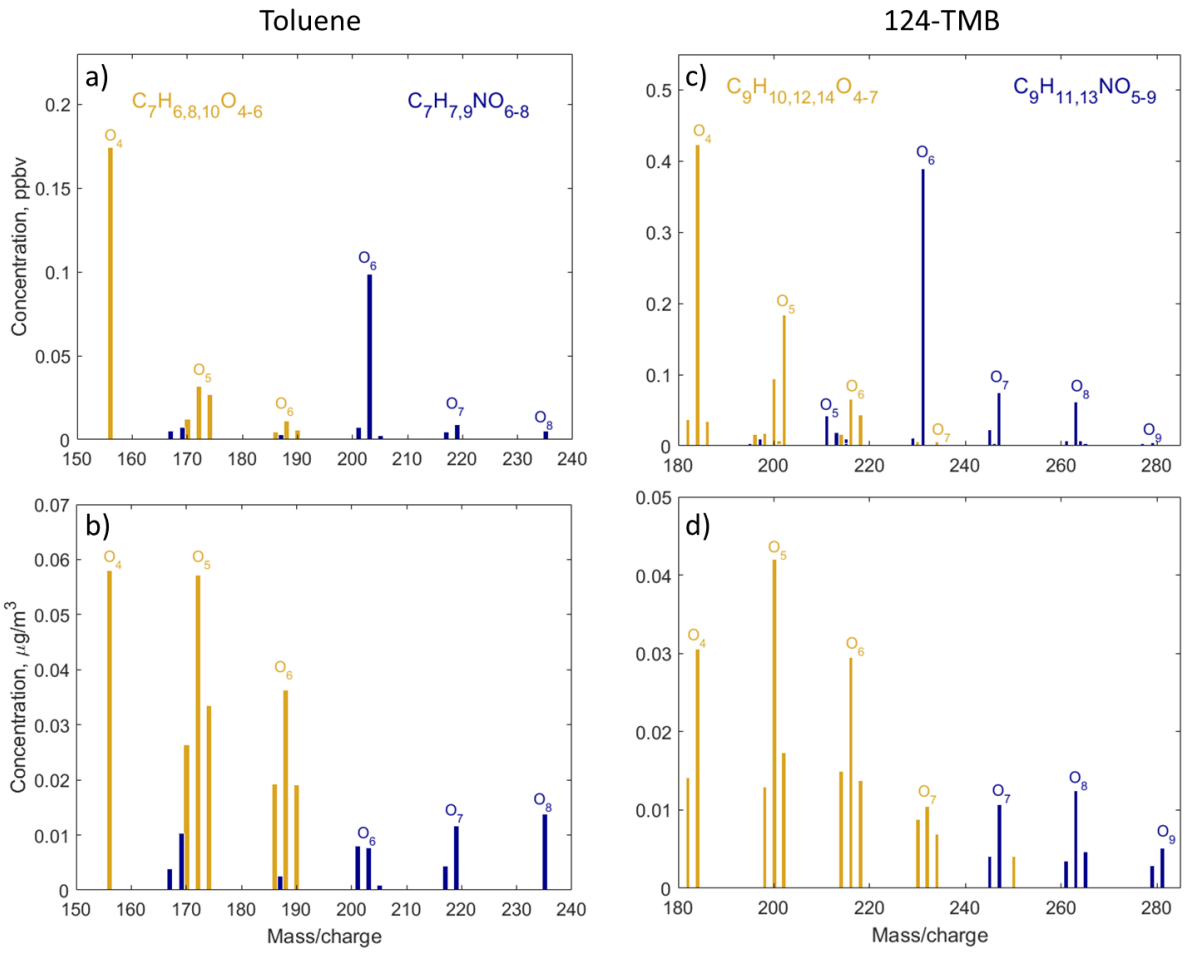

Figure 4: Mass spectra of compounds with high oxygen content (O:C > 0.44) from toluene (panels a and b) and 1,2,4-trimethylbenzene (panels c and d) detected by NH_4^+ CIMS. Gas-phase mass spectra are shown in the upper panels (a) and (c), and particle-phase mass spectra are shown in bottom panels (b) and (d). Non-nitrogen-containing compounds are shown in yellow, and nitrogen-containing compounds are shown in blue.

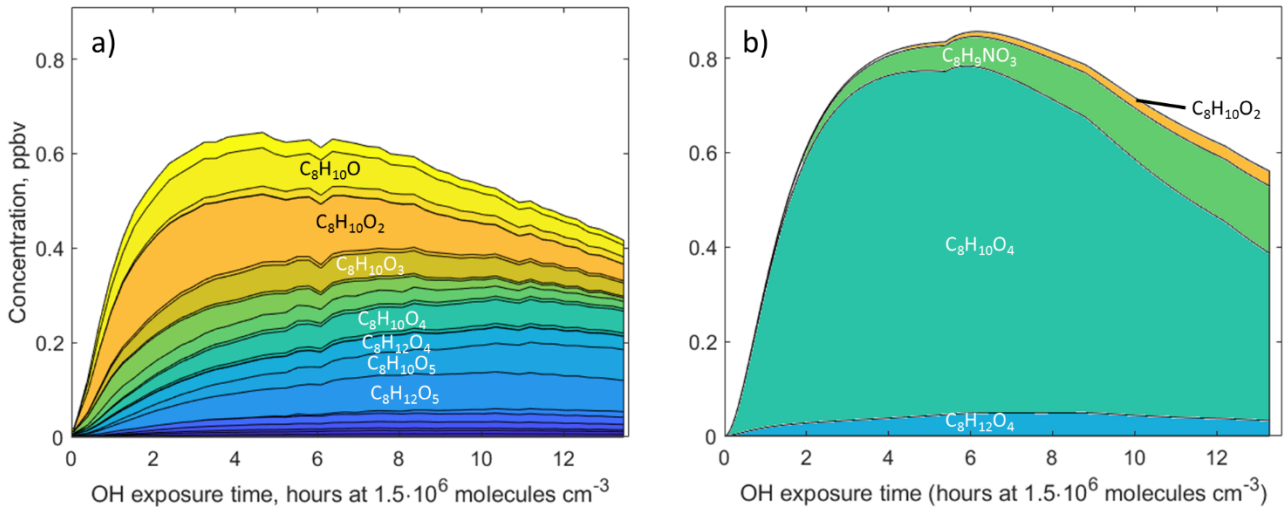

Figure 5: C_8 gas-phase products (a) detected by PTR-MS and NH_4^+ CIMS and (b) predicted by MCM v3.3.1 during oxidation of 1,2,4-trimethylbenzene.

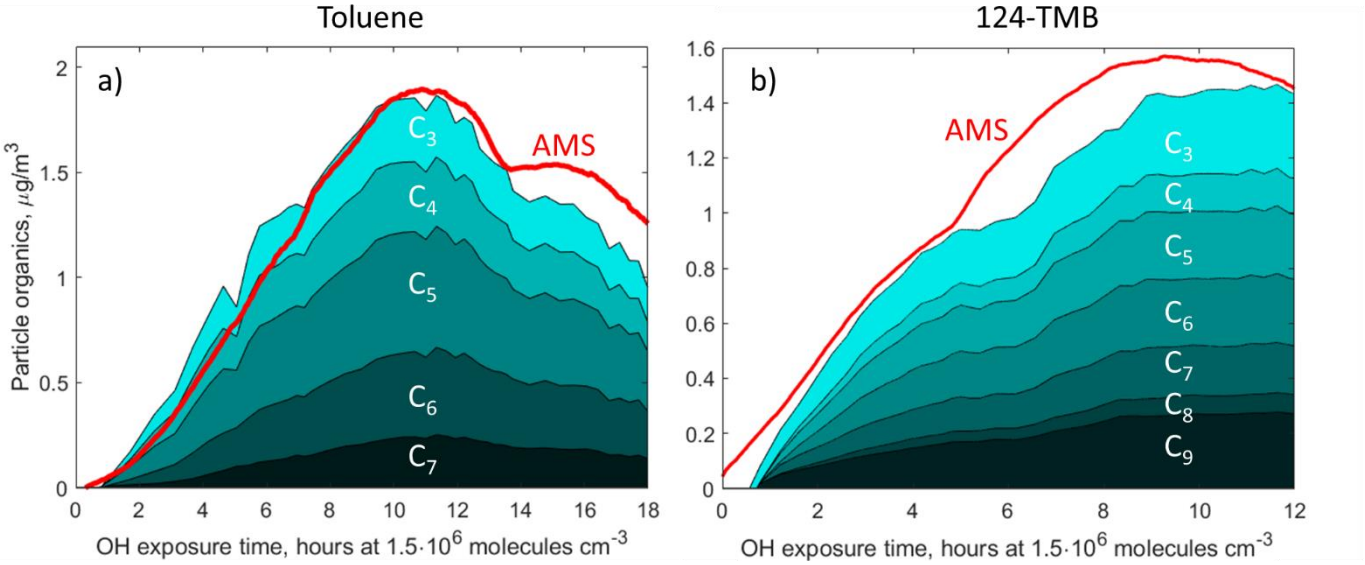

Figure 6: Total organics measured in the particle phase by NH_4^+ CIMS and binned by the carbon atom number (a) in the toluene ~~124-TMB~~ photooxidation experiment and (b) the 1,2,4-TMB ~~toluene~~ photooxidation experiment. Total carbon measured by AMS is in red.